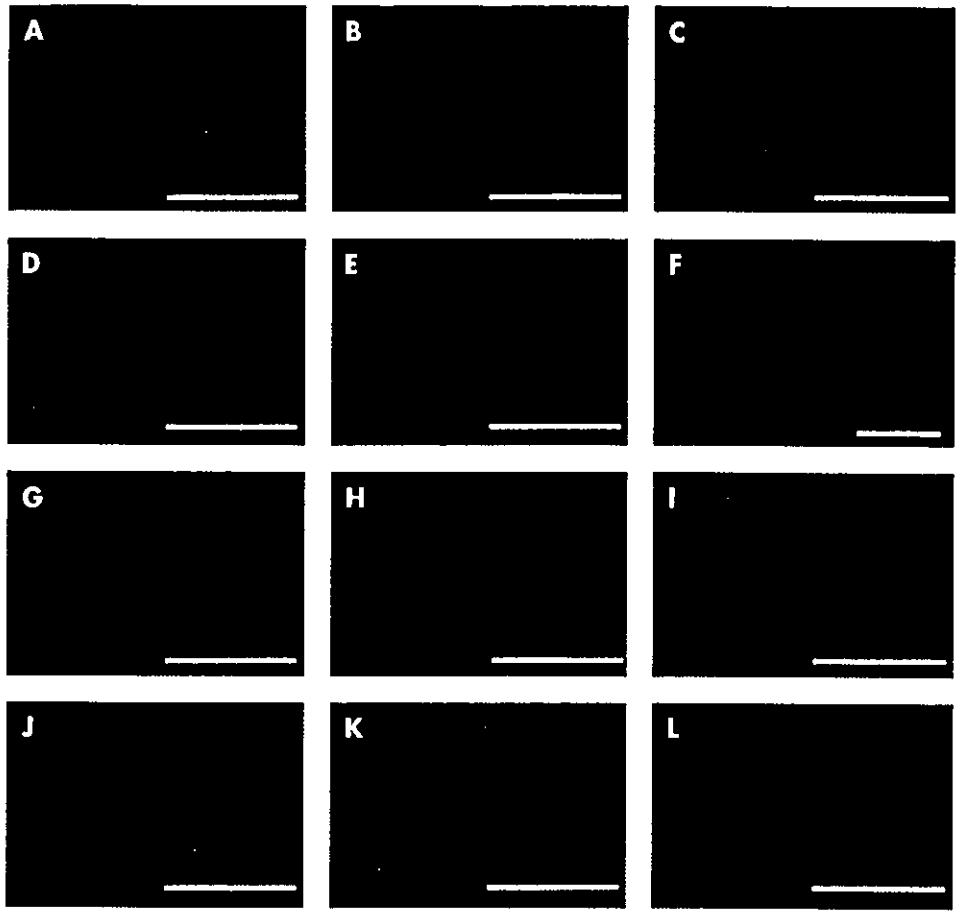

Figure 2 Expression of matrix metalloproteinases in CD14 positive monocytes, TRAP positive mononuclear cells (TPMoC), and TRAP positive multinucleated cells (TPMuC) as demonstrated by immunocytochemical analysis. MMP-2, MMP-9, MMP-12, and MMP-14 were expressed by TPMuC (C, F, I, and L), while additional expression of MMP-2 and MMP-9 was seen in TPMoC (B and E). (A, D, G, and J) CD14 positive monocytes; (B, E, H, and K) TPMoC; (C, F, I, and L) TPMuC. (A, B, and C) MMP-2; (D, E, and F) MMP-9; (G, H, and I) MMP-12; (J, K, and L) MMP-14. Bar = 100 μm in A, D, G, and J; bar = 50 μm in B, C, E, F, H, I, K, and L.

saline (PBS) plus 0.2% Triton X100 and 1% bovine serum albumin for 30 minutes, 2 μg/ml of the primary antibody for the corresponding protein (MMP-2, MMP-14: Fuji Chem, Toyama, Japan; MMP-9: Santa Cruz, Santa Cruz, CA; MMP-12, Genzyme) in PBS (or isotype matched antibody as a negative control) at a similar concentration for one hour, and then 1 μg/ml of the secondary antibody in PBS for one hour. As the secondary antibody, rhodamine conjugated rabbit antimouse immunoglobulins (Dako, Glostrup, Denmark) were used for MMP-2, MMP-12, or MMP-14, while FITC conjugated rabbit antigoat IgG (Santa Cruz) was used for MMP-9. Finally, the slides were cover slipped with PBS-glycerol containing an antifading agent (*p*-phenylenediamine dihydrochloride; Sigma) and were observed under a fluorescent microscope (E800; Nikon, Tokyo, Japan) equipped with a standard mercury lamp.

Immunohistochemistry

Immunohistochemical staining was performed by the streptavidin biotin-peroxidase complex technique using a Histofine SAB-PO kit (Nichirei, Tokyo, Japan) according to the manufacturer's instructions. Briefly, after blocking endogenous peroxidase and non-specific antigens, primary antibodies were applied to tissue sections and incubated for 24 hours at 4°C to detect MMP-2, MMP-9, MMP-12, and MMP-14. Isotype matched antibodies were used for the negative controls. After washing in PBS, the sections were incubated with the secondary antibody for 20 minutes at room temperature, followed by incubation with peroxidase conjugated streptavidin (Nichirei) for 20 minutes at room temperature and washing in PBS. Finally, colour was developed using 3,3'-diaminobenzidine tetrahydrochloride (Dojindo Laboratories, Kumamoto, Japan), and the sections were counterstained with haematoxylin.

Immunohistochemical staining for MMPs combined with TRAP staining

Immunohistochemical staining for MMPs combined with TRAP staining was performed using the streptavidin biotin-alkaline phosphatase complex technique (Nichirei) according to the method recommended by the manufacturer. Briefly, after blocking non-specific antigenicity, primary antibodies were applied to the tissue sections and incubated for 24 hours at 4°C to detect MMP-2 and MMP-9. Isotype matched antibodies were used as the negative controls. After washing in Tris-buffered saline (TBS), the sections were incubated with the secondary antibody for 20 minutes at room temperature, followed by incubation with alkaline phosphatase conjugated streptavidin (Nichirei) for 10 minutes at room temperature and washing in TBS. Finally, colour was developed using a fast blue substrate kit (Nichirei). Endogenous alkaline phosphatase activity was blocked using an alkaline phosphatase blocking reagent (levamisole; DAKO). After immunostaining, TRAP staining was performed with a commercial acid phosphatase leucocyte kit (Sigma).

TRAP enzyme staining

TRAP enzyme was detected in paraffin sections using a commercial acid phosphatase leucocyte kit (Sigma).

Quantification of MMP-2 and MMP-9

The concentrations of MMP-2 and MMP-9 in culture supernatants were measured using an enzyme linked immunosorbent assay (ELISA) kit (BIOTRAK; Amersham Pharmacia Biotech, Piscataway, NJ) according to the manufacturer's instructions.

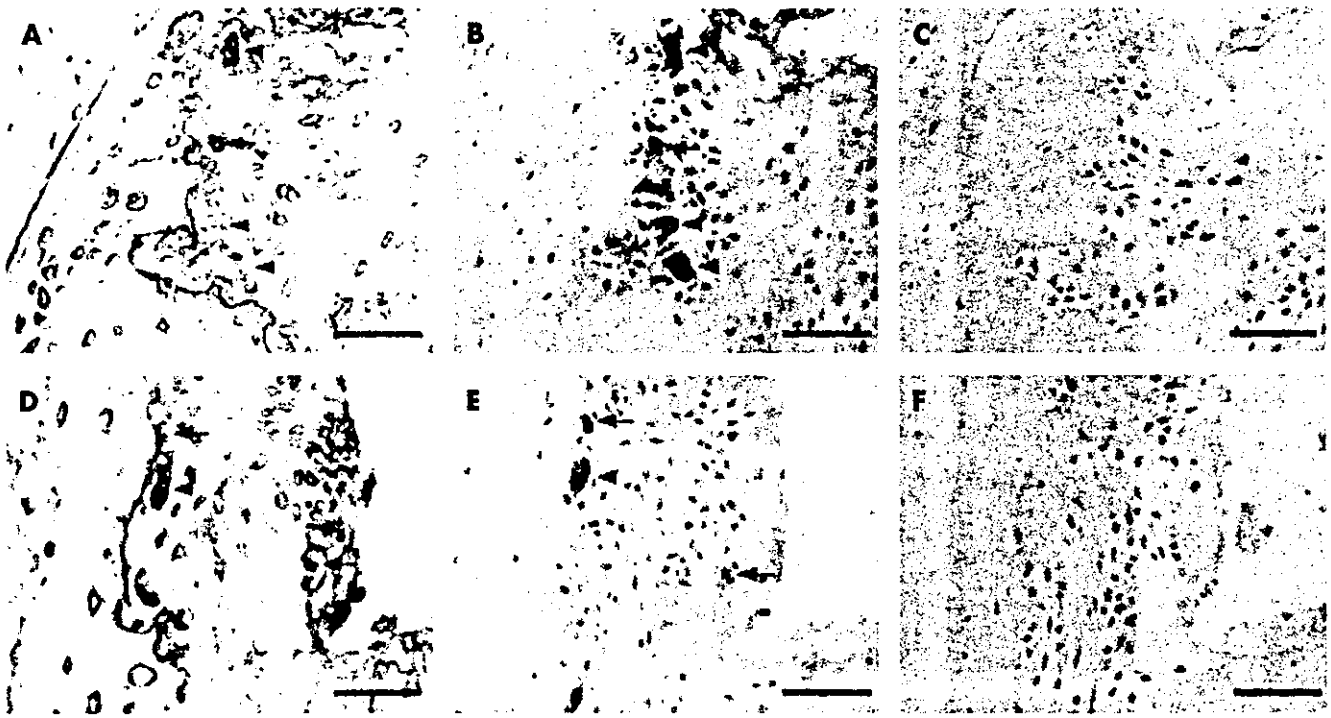

Figure 3 Immunolocalisation of MMP-2 and MMP-9 in RA synovial tissue at the bone-cartilage interface. (A and D) TRAP staining, serial section. Mononuclear (arrows) and multinucleated cells (arrowheads) in RA synovial tissue at the bone-cartilage interface display TRAP activity. (B and E) Immunohistochemistry for MMP-2 and MMP-9. The TRAP positive mononuclear and multinucleated cells shown in A and D express MMP-2 and MMP-9. (C and F) Isotype controls for B and E. Haematoxylin counterstaining was performed in B, C, E, and F. Bar = 100 μm.

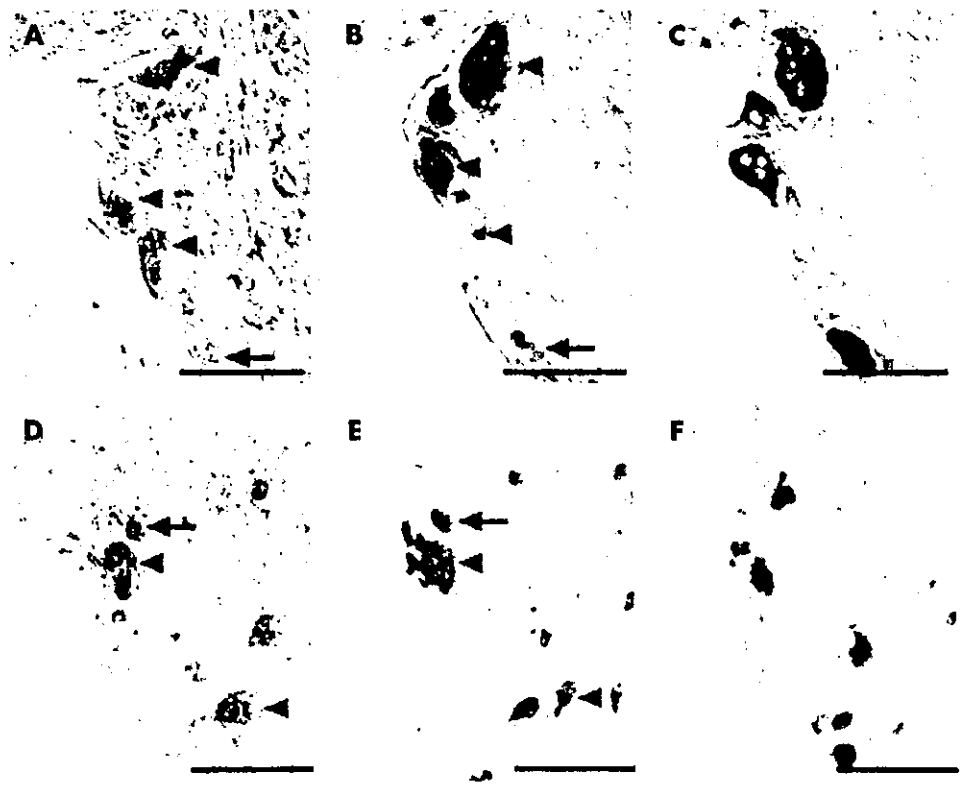

Figure 4 Immunostaining for MMP-2 or MMP-9 combined with TRAP staining of RA synovial tissue at the bone-cartilage interface. (A and D) Immunostaining for MMP-2 or MMP-9. Mononuclear cells (arrows) and multinucleated cells (arrowheads) in RA synovial tissue at the bone-cartilage interface express MMP-2 and MMP-9. (B and E) Immunostaining for MMP-2 or MMP-9 combined with TRAP staining. The TRAP positive cells are positive for MMP-2 and MMP-9. (C and F) Isotype controls for A and D combined with TRAP staining. Bar = 50 μm.

Cartilage degradation assay

The cartilage degradation assay was originally described by Steinberg *et al*,[23] and was reported by Janusz *et al* and Scott.[24 25] Briefly, degradation of cartilage by TRAP positive mononuclear cells was assessed by culturing those cells in the presence of a radiolabelled cartilage disc. Cartilage discs were prepared from bovine nasal septal tissues (obtained at the time of slaughter) using a 4 mm cork bore. Radiolabelling of the discs was done with ^{35}S labelled Na_2SO_4 in the manner described by Janusz *et al* and the discs contained 5.0×10^{4}–

2.0×10^5 dpm of ^{35}S. The discs were then subjected to five freeze-thaw cycles and heated at 65°C for 15 minutes to inactivate endogenous enzymes and cytokines, after which discs were stored at −20°C before use.

Before performing the cartilage degradation assay, the discs were treated with DMEM (Gibco BRL) containing 0.4% collagenase I (Sigma) for 30 minutes at 37°C and were washed with DMEM containing 10% FCS. TRAP positive mononuclear cells (1.0×10^5) were added to each well of a 96 well culture plate and were cultured on the radiolabelled discs for seven days in 200 µl of medium. For the neutralisation assay, 10 µM and 100 µM concentrations of an MMP-2/9 inhibitor (CALBIOCHEM; San Diego, CA) were added to the medium. Specific inhibition of both MMP-2 and MMP-9 at these concentrations by this inhibitor has been reported.[36] On day 7, 200 µl of supernatant was removed from each well, added to 3 ml of ready-safe scintillation fluid (Beckman Instruments, Fullerton, CA), and counted in a scintillation counter (Quanta Smart for the Tricarb Liquid Scintillation Analyser; Packard Instrument Company, Merdin, CT). Then the residual isotope in each cartilage disc was measured in the same manner after the disc had been completely digested using 0.5 ml of tissue solubiliser (Beckman Instruments). The percentage of ^{35}S release into the supernatant was calculated using the following formula:

$$100 \times (\text{dpm in supernatant})/(\text{dpm in supernatant} + \text{disc})$$

All experiments were performed in triplicate.

RESULTS

Detection of TRAP positive cells in RA synovium near the cartilage-bone interface

Histological examination of the bone-cartilage interface was performed. The synovium adjacent to the bone-cartilage interface was found to contain TRAP positive cells. Table 3 gives details of the number of TRAP positive cells.

TRAP positive mononuclear and multinucleated cells induced from peripheral blood monocytes by culture with RA synoviocytes express various MMPs

TRAP positive mononuclear and multinucleated cells were induced by coculture of peripheral blood monocytes with RA synoviocytes. We also performed coculture with RA synovial macrophages obtained from four patients with RA and RA synovial fibroblasts by the same method. However, most of the synovial macrophages disappeared within two weeks. Then MMP mRNA expression by the TRAP positive cells was assessed using RT-PCR and northern blot analysis. RT-PCR demonstrated that peripheral blood monocytes contained mRNA for MMP-8 and MMP-14 (fig 1A). In TRAP positive mononuclear and multinucleated cells, additional expression of the mRNAs for MMP-1, MMP-2, MMP-3, MMP-7, MMP-9, MMP-10, and MMP-12 was detected. Northern blot analysis showed that the expression of MMP-2, MMP-9, MMP-12, and MMP-14 was increased in TRAP positive mononuclear and multinucleated cells (fig 1B). Although MMP-2 expression was significantly increased in TRAP positive mononuclear cells, MMP-9 and MMP-12 expression was higher in TRAP positive multinucleated cells. Expression of MMP-14 was similar in the two cell phenotypes. The amount of mRNA applied to each lane did not differ significantly, as determined by monitoring 28S ribosomal RNA. Other MMPs were not detectable by northern blot analysis (data not shown).

Immunocytochemical analysis of MMP-2, MMP-9, MMP-12, and MMP-14 was performed to confirm the expression of MMP proteins using monoclonal or polyclonal antibodies specific for these MMPs (fig 2). MMP-2 and MMP-9 were demonstrated in TRAP positive mononuclear cells, while additional expression of MMP-12 and MMP-14 was seen in TRAP positive multinucleated cells. These results were similar to those obtained by northern blot analysis. The other MMPs were not detected in monocytes or TRAP positive cells.

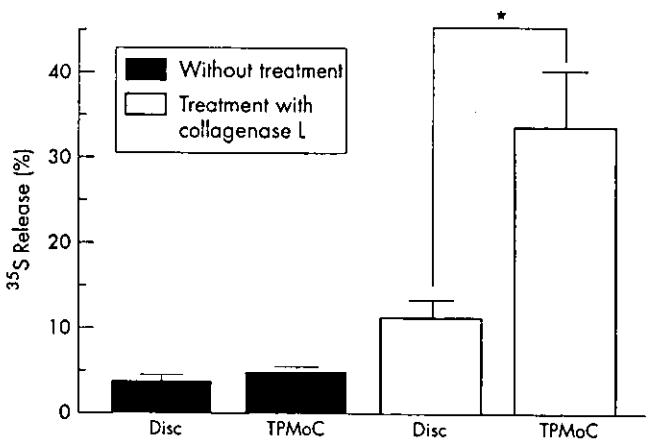

Figure 5 Degradation of cartilage by TRAP positive mononuclear cells (TPMoC). Bars show the mean percentage and SD of ^{35}S release on day 7 in 10 replicate cultures when radiolabelled cartilage discs were cultured in the presence (TPMoC) or absence of TPMoC (disc). The percentage degradation with and without collagenase I pretreatment is shown. *$p<0.01$ for disc v TPMoC (Mann-Whitney test).

TRAP positive mononuclear and multinucleated cells in RA synovial tissue at the bone-cartilage interface express MMP-2 and MMP-9

We examined MMP-2, MMP-9, MMP-12, and MMP-14 expression in the synovial tissue of 10 patients with RA by immunohistochemistry (fig 3). To detect the co-localisation of TRAP positive cells and MMP, we performed immunoalkaline phosphatase staining for a single MMP combined with TRAP staining in the same tissue section (fig 4). TRAP positive mononuclear and multinucleated cells in RA synovial tissue at the bone-cartilage interface showed strong expression of MMP-2 and MMP-9. Some of the synoviocytes at the bone-cartilage interface were also stained, but were only weakly positive. We did not detect MMP-12 or MMP-14 expression in RA synovial tissue (data not shown).

TRAP positive mononuclear cells have the potential to induce the degradation of cartilage matrix by MMP-2 and MMP-9

We examined whether TRAP positive mononuclear cells induced from monocytes by culture with RA synoviocytes had the potential to destroy cartilage. Release of ^{35}S from labelled cartilage discs was increased in the supernatants of cultures containing TRAP positive mononuclear cells when compared with supernatants from cultures without these cells (fig 5). However, TRAP positive mononuclear cells did not induce degradation of cartilage discs without collagenase pretreatment. In the culture supernatants of TRAP positive mononuclear cells, high concentrations of MMP-2 and MMP-9 were detected (fig 6). When neutralisation experiments were performed using an MMP-2 and MMP-9 inhibitor to assess whether MMP-2 or MMP-9 released by TRAP positive mononuclear cells was responsible for induced cartilage degradation, it was found that degradation was completely inhibited by 100 µmol/l of the inhibitor (fig 7). These results suggest that TRAP positive cells induced from peripheral blood monocytes by culture with RA synoviocytes have the potential to induce cartilage degradation by MMP-2 and MMP-9.

DISCUSSION

In this study we clearly demonstrated that TRAP positive mononuclear and multinucleated cells exist in RA synovial tissue at the bone-cartilage interface and that these cells expressed MMP-2 (gelatinase A) and MMP-9 (gelatinase B). We also showed that TRAP positive mononuclear and multinucleated cells induced from peripheral blood monocytes by culture with RA synoviocytes expressed various

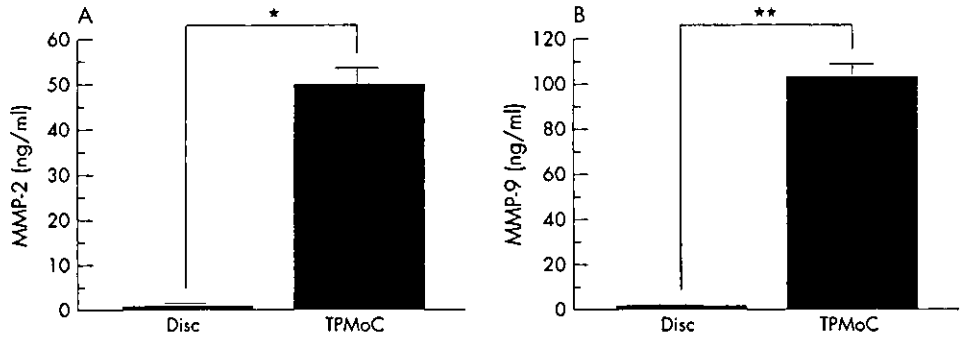

Figure 6 Secretion of MMP-2 (A) and MMP-9 (B) into culture supernatant on day 7 in 10 replicate cultures when radiolabelled cartilage discs were incubated in the presence of TRAP positive mononuclear cells (TPMoC) or in the absence of such cells (disc). *, **p<0.01 for disc v TPMoC (Mann-Whitney test).

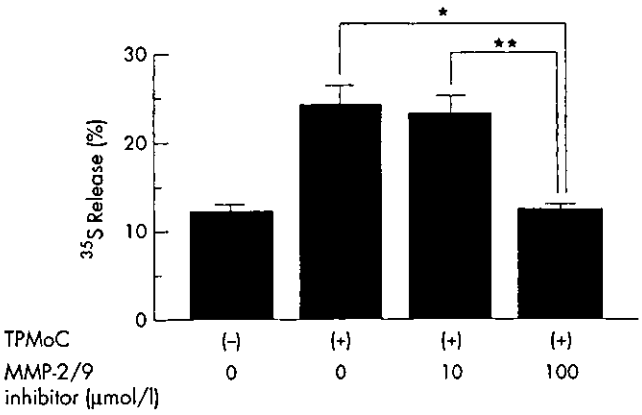

Figure 7 A neutralisation experiment in the cartilage degradation assay was performed by adding a blocking agent for MMP-2 and MMP-9 to cultures of TRAP positive mononuclear cells. The inhibitor (100 μmol/l) blocked cartilage degradation. The mean percentage and SD shown in each column were calculated from 10 values of two identical experiments. *, **p<0.01 for 0 μmol/l v 100 μmol/l and 10 μmol/l v 100 μmol/l (Mann-Whitney test).

MMPs, especially MMP-2 and MMP-9, and that these generated mononuclear cells could cause cartilage degradation by producing MMP-2 and MMP-9. As far as we know, this is the first demonstration of cartilage degradation by TRAP positive cells from patients with RA.

We were aware of the aggregation of TRAP positive mononuclear and multinucleated cells in RA synovial tissues adjacent to areas of cartilage destruction, based on histological examination, and proposed that these cells might play some part in the destruction of articular cartilage.

First, we examined the expression of mRNAs for various MMPs by TRAP positive mononuclear and multinucleated cells induced from peripheral blood monocytes by coculture with RA synoviocytes. We found that TRAP positive mononuclear and multinucleated cells expressed mRNAs for a number of MMPs by RT-PCR, including MMP-1 (fibroblast-type collagenase), MMP-2, MMP-3 (stromelysin-1), MMP-7 (matrilysin), MMP-8 (neutrophil-type collagenase), MMP-9, MMP-10 (stromelysin-2), MMP-12 (macrophage metalloelastase), and MMP-14 (MT1-MMP). Northern blot analysis also detected some MMPs, including MMP-2, MMP-9, MMP-12, and MMP-14. Investigation of MMP protein expression by immunocytochemistry showed that MMP-2 and MMP-9 were expressed in both mononuclear and multinucleated cells, but MMP-12 and MMP-14 were only expressed in multinucleated cells. Discrepancies of mRNA and protein expression among the results of RT-PCR, northern blot analysis, and immunocytochemistry were observed. Variations in the sensitivity of the three methods and post-transcriptional regulation might have caused these discrepancies. However, clearly, TRAP positive cells generated in vitro had the potential to produce many kinds of MMPs. We also examined MMP expression in RA synovial tissue adjacent to sites of cartilage destruction. Only MMP-2 and MMP-9 were detected in TRAP positive cells in vivo. Further investigation of MMP expression by TRAP positive cells is necessary, but we have shown that MMP-2 and MMP-9 may play a part in the tissue destruction that occurs in RA.

MMP-9 has been reported to be localised in monocytes/macrophages and osteoclasts.[27 28] In this study MMP-9 mRNA and protein were detected in TRAP positive mononuclear and multinucleated cells both in vitro and in vivo. These findings were consistent with a previous report.[6] Production of MMP-2 by osteoclasts is controversial. Previously, osteoclasts were reported to produce MMP-2,[16] but Ovejero *et al* recently reported that osteoclasts from rabbits did not express MMP-2.[29] It was also shown that MMP-2 can bind to $\alpha_v\beta_3$ integrin and that MMP-2 produced by osteoblasts or other cells only binds to $\alpha_v\beta_3$ integrin expressed by osteoclasts.[30] However, the present study showed that TRAP positive mononuclear and multinucleated cells expressed mRNA for MMP-2, these cells were stained positive by immunocytochemistry for MMP-2, and ELISA showed that mononuclear cells secreted MMP-2 into culture supernatants. Interestingly, MMP-2 expression was significantly up regulated in TRAP positive mononuclear cells in comparison with multinucleated cells. Further investigation is still necessary, but we believe that TRAP positive mononuclear cells and multinucleated cells can produce MMP-2.

MMP-2 and MMP-9 are gelatinases and seem to play a part in soft tissue destruction, but collagenases and stromelysin are also necessary for complete cartilage destruction. In the cartilage degradation assay, pretreatment with collagenase was necessary to allow cartilage degradation by TRAP positive mononuclear cells. Cooperation with synoviocytes and chondrocytes may be important in the mechanism of in vivo tissue degradation.

We previously reported that osteoclastogenesis was enhanced in the iliac bone marrow of patients with RA and that this was a possible cause of generalised osteoporosis.[31] Because TRAP positive mononuclear and multinucleated cells were identified in RA synovium,[15] we speculated that synovial fibroblasts participated in TRAP positive cell recruitment and in degradation of the osteochondral matrix. Therefore, we established a system to generate osteoclast-like cells from peripheral blood monocytes by culture with RA synoviocytes.[20] Recently, others have reported osteoclastogenesis when RA synovial macrophages and healthy peripheral blood mononuclear cells are cocultured with RA synovial fibroblasts.[32-34]

Our study showed some differences between TRAP positive cells in RA synovial tissue and TRAP positive cells generated in vitro. When generated in vitro, the TRAP positive mononuclear cells mainly expressed MMP-2 and MMP-9, and showed the same pattern of expression as TRAP positive mononuclear

cells detected in synovial tissue. In contrast, the in vitro generated TRAP positive multinucleated cells expressed MMP-2, MMP-9, MMP-12, and MMP-14, while the TRAP positive multinucleated cells in RA synovial tissue were only positive for MMP-2 and MMP-9. The sensitivity of immunocytochemistry might be different from that of immunohistochemistry, but the characteristics of in vitro and in vivo TRAP positive cells should be investigated further.

RA synovial fluid contains high levels of MMP-1, MMP-2, MMP-3, MMP-8, and MMP-9, which have been implicated in cartilage destruction.[9] The major source of these proteins may be the synovium, where many kinds of MMP mRNAs have been detected.[10] However, considering that joint destruction progresses in a focal fashion, the proteolytic activity of RA synovial fluid, which bathes the entire joint, is not sufficient to explain the pathology of this disease. At the cartilage-synovial interface, where focal cartilage and bone destruction occurs, enhanced osteoclastogenesis has been observed.[15] In this study we also demonstrated focal aggregation of TRAP positive mononuclear and multinucleated cells at sites of destruction and positive staining of these cells for MMP-2 and MMP-9. Interestingly, TRAP positive mononuclear cells induced cartilage destruction in vitro by expressing MMP-2 and MMP-9.

MMP-9 expression by TRAP positive mononuclear cells suggested their phenotypic similarity with chondroclasts, which have been identified at the growth plate bone-cartilage interface.[17] We have already shown that in vitro generated TRAP positive multinucleated cells possess the characteristics of osteoclasts.[20] Blocking of this chondroclast-like and osteoclast-like cell lineage, the generation of which is mediated by RA synoviocytes, may be a possible way to prevent joint destruction in RA.

ACKNOWLEDGEMENTS

We greatly appreciate the invaluable technical assistance of H Oku and K Asai.

Authors' affiliations
H Tsuboi, Y Matsui, K Hayashida, A Nampei, J Hashimoto, H Yoshikawa, T Ochi, Department of Orthopaedic Surgery, Osaka University Graduate School of Medicine, Osaka, Japan
S Yamane, M Maeda-Tanimura, R Suzuki, Department of Immunology, Shionogi Research Laboratories, Shionogi and Co, Ltd, Osaka, Japan

REFERENCES

1 **Gravallese EM**, Harada Y, Wang JT, Gorn AH, Thornhill TS, Goldring SR. Identification of cell types responsible for bone resorption in rheumatoid arthritis and juvenile rheumatoid arthritis. Am J Pathol 1998;152:943–51.
2 **Tak PP**, Bresnihan B. The pathogenesis and prevention of joint damage in rheumatoid arthritis: advances from synovial biopsy and tissue analysis. Arthritis Rheum 2000;43:2619–33.
3 **Suda T**, Kobayashi K, Jimi E, Udagawa N, Takahashi N. The molecular basis of osteoclast differentiation and activation. Novartis Found Symp 2001;232:235–47; discussion 247–50.
4 **Azuma Y**, Kaji K, Katogi R, Takeshita S, Kudo A. Tumor necrosis factor-alpha induces differentiation of and bone resorption by osteoclasts. J Biol Chem 2000;275:4858–64.
5 **Scheven BA**, Milne JS, Hunter I, Robins SP. Macrophage-inflammatory protein-1alpha regulates preosteoclast differentiation in vitro. Biochem Biophys Res Commun 1999;254:773–8.
6 **Okada Y**, Naka K, Kawamura K, Matsumoto T, Nakanishi I, Fujimoto N, *et al*. Localization of matrix metalloproteinase 9 (92-kilodalton gelatinase/type IV collagenase = gelatinase B) in osteoclasts: implications for bone resorption. Lab Invest 1995;72:311–22.
7 **Kaneko M**, Tomita T, Nakase T, Ohsawa Y, Seki H, Takeuchi E, *et al*. Expression of proteinases and inflammatory cytokines in subchondral bone regions in the destructive joint of rheumatoid arthritis. Rheumatology (Oxford) 2001;40:247–55.
8 **Lindy O**, Konttinen YT, Sorsa T, Ding Y, Santavirta S, Ceponis A, *et al*. Matrix metalloproteinase 13 (collagenase 3) in human rheumatoid synovium. Arthritis Rheum 1997;40:1391–9.
9 **Cunnane G**, FitzGerald O, Hummel KM, Gay RE, Gay S, Bresnihan B. Collagenase, cathepsin B and cathepsin L gene expression in the synovial membrane of patients with early inflammatory arthritis. Rheumatology (Oxford) 1999;38:34–42.
10 **Konttinen YT**, Ainola M, Valleala H, Ma J, Ida H, Mandelin J, *et al*. Analysis of 16 different matrix metalloproteinases (MMP-1 to MMP-20) in the synovial membrane: different profiles in trauma and rheumatoid arthritis. Ann Rheum Dis 1999;58:691–7.
11 **Konttinen YT**, Salo T, Hanemaaijer R, Valleala H, Sorsa T, Sutinen M, *et al*. Collagenase-3 (MMP-13) and its activators in rheumatoid arthritis: localization in the pannus-hard tissue junction and inhibition by alendronate. Matrix Biol 1999;18:401–12.
12 **Lotz M**, Hashimoto S, Kuhn K. Mechanisms of chondrocyte apoptosis. Osteoarthritis Cartilage 1999;7:389–91.
13 **Tetlow LC**, Adlam DJ, Woolley DE. Matrix metalloproteinase and proinflammatory cytokine production by chondrocytes of human osteoarthritic cartilage: associations with degenerative changes. Arthritis Rheum 2001;44:585–94.
14 **Fujikawa Y**, Shingu M, Torisu T, Itonaga I, Masumi S. Bone resorption by tartrate-resistant acid phosphatase-positive multinuclear cells isolated from rheumatoid synovium. Br J Rheumatol 1996;35:213–17.
15 **Gravallese EM**, Manning C, Tsay A, Naito A, Pan C, Amento E, *et al*. Synovial tissue in rheumatoid arthritis is a source of osteoclast differentiation factor. Arthritis Rheum 2000;43:250–8.
16 **Delaisse JM**, Engsig MT, Everts V, del Carmen Ovejero M, Ferreras M, Lund L, *et al*. Proteinases in bone resorption: obvious and less obvious roles. Clin Chim Acta 2000;291:223–34.
17 **Vu TH**, Shipley JM, Bergers G, Berger JE, Helms JA, Hanahan D, *et al*. MMP-9/gelatinase B is a key regulator of growth plate angiogenesis and apoptosis of hypertrophic chondrocytes. Cell 1998;93:411–22.
18 **Arnett FC**, Edworthy SM, Bloch DA, McShane DJ, Fries JF, Cooper NS, *et al*. The American Rheumatism Association 1987 revised criteria for the classification of rheumatoid arthritis. Arthritis Rheum 1988;31:315–24.
19 **Kaneko M**, Tomita T, Nakase T, Takeuchi E, Iwasaki M, Sugamoto K, *et al*. Rapid decalcification using microwaves for in situ hybridization in skeletal tissues. Biotech Histochem 1999;74:49–54.
20 **Toyosaki-Maeda T**, Takano H, Tomita T, Tsuruta Y, Maeda-Tanimura M, Shimaoka Y, *et al*. Differentiation of monocytes into multinucleated giant bone-resorbing cells: two-step differentiation induced by nurse-like cells and cytokines. Arthritis Res 2001;3:306–10.
21 **Takeuchi E**, Tomita T, Toyosaki-Maeda T, Kaneko M, Takano H, Hashimoto H, *et al*. Establishment and characterization of nurse cell-like stromal cell lines from synovial tissues of patients with rheumatoid arthritis. Arthritis Rheum 1999;42:221–8.
22 **Church GM**, Gilbert W. Genomic sequencing. Proc Natl Acad Sci USA 1984;81:1991–5.
23 **Steinberg J**, Tsukamoto S, Sledge CB. A tissue culture model of cartilage breakdown in rheumatoid arthritis. III. Effects of antirheumatic drugs. Arthritis Rheum 1979;22:877–85.
24 **Janusz MJ**, Hare M. Cartilage degradation by cocultures of transformed macrophage and fibroblast cell lines. A model of metalloproteinase-mediated connective tissue degradation. J Immunol 1993;150:1922–31.
25 **Scott BB**, Weisbrot LM, Greenwood JD, Bogoch ER, Paige CJ, Keystone EC. Rheumatoid arthritis synovial fibroblast and U937 macrophage/monocyte cell line interaction in cartilage degradation. Arthritis Rheum 1997;40:490–8.
26 **Koivunen E**, Arap W, Valtanen H, Rainisalo A, Medina OP, Heikkila P, *et al*. Tumor targeting with a selective gelatinase inhibitor. Nat Biotechnol 1999;17:768–74.
27 **Zhang Y**, McCluskey K, Fujii K, Wahl LM. Differential regulation of monocyte matrix metalloproteinase and TIMP-1 production by TNF-alpha, granulocyte-macrophage CSF, and IL-1 beta through prostaglandin-dependent and -independent mechanisms. J Immunol 1998;161:3071–6.
28 **Jovanovic DV**, Martel-Pelletier J, Di Battista JA, Mineau F, Jolicoeur FC, Benderdour M, *et al*. Stimulation of 92-kd gelatinase (matrix metalloproteinase 9) production by interleukin-17 in human monocyte/macrophages: a possible role in rheumatoid arthritis. Arthritis Rheum 2000;43:1134–44.
29 **Ovejero M**, Lenhard T, Bayer L, Foged N, Delaisse J. Systemic search for MMP expression in osteoclasts [abstract]. Bone 1998;23:S548.
30 **Brooks PC**, Stromblad S, Sanders LC, von Schalscha TL, Aimes RT, Stetler-Stevenson WG, *et al*. Localization of matrix metalloproteinase MMP-2 to the surface of invasive cells by interaction with integrin alpha v beta 3. Cell 1996;85:683–93.
31 **Toritsuka Y**, Nakamura N, Lee SB, Hashimoto J, Yasui N, Shino K, *et al*. Osteoclastogenesis in iliac bone marrow of patients with rheumatoid arthritis. J Rheumatol 1997;24:1690–6.
32 **Itonaga I**, Fujikawa Y, Sabokbar A, Murray DW, Athanasou NA. Rheumatoid arthritis synovial macrophage-osteoclast differentiation is osteoprotegerin ligand-dependent. J Pathol 2000;192:97–104.
33 **Shigeyama Y**, Pap T, Kunzler P, Simmen BR, Gay RE, Gay S. Expression of osteoclast differentiation factor in rheumatoid arthritis. Arthritis Rheum 2000;43:2523–30.
34 **Takayanagi H**, Iizuka H, Juji T, Nakagawa T, Yamamoto A, Miyazaki T, *et al*. Involvement of receptor activator of nuclear factor kappaB ligand/osteoclast differentiation factor in osteoclastogenesis from synoviocytes in rheumatoid arthritis. Arthritis Rheum 2000;43:259–69.
35 **Yoshihara Y**, Nakamura H, Obata K, Yamada H, Hayakawa T, Fujikawa K, *et al*. Matrix metalloproteinases and tissue inhibitors of metalloproteinases in synovial fluids from patients with rheumatoid arthritis or osteoarthritis. Ann Rheum Dis 2000;59:455–61.

Rheumatology 2003;42:353-356
doi:10.1093/rheumatology/keg088, available online at www.rheumatology.oupjournals.org

Novel autoantibodies to pituitary gland specific factor 1a in patients with rheumatoid arthritis

S. Tanaka, K. Tatsumi, T. Tomita[1], M. Kimura, T. Takano, H. Yoshikawa[1] and N. Amino

Objective. **We recently identified a new protein, pituitary gland specific factor 1a (PGSF1a), that is specifically transcribed in the pituitary gland. In our investigation of anti-PGSF1a antibody for pituitary diseases, we examined it in patients with RA and other autoimmune diseases. We unexpectedly discovered the frequent existence of anti-PGSF1a antibody in patients with RA. We therefore examined the prevalence of this antibody to understand its clinical significance in RA.**

Methods. **Anti-PGSF1a antibody was detected by radioligand assay using recombinant ^{35}S-labelled PGSF1a protein. Antibody activity is expressed as an index that was obtained by comparison with normal pooled serum.**

Results. **RA patients had a significantly higher mean anti-PGSF1a antibody index ($n=46$, 1.28 ± 0.38, $P < 0.001$) than healthy controls ($n=36$, 1.04 ± 0.13). Indices greater than the cut-off value (mean+2 S.D. of healthy controls) were found in 43.5% (20/46) and 10.0% (2/20) of patients with RA and osteoarthritis, respectively. There was no correlation between the activities of anti-PGSF1a antibodies and titres of rheumatoid factor (RF) or serum C-reactive protein concentrations, but RA patients with more erosive disease had a higher mean anti-PGSF1a antibody index. Four of eight sera samples obtained from RF-negative RA patients were positive for anti-PGSF1a antibodies.**

Conclusion. **Anti-PGSF1a antibody is a useful new marker for the diagnosis of RA, especially for RF-negative RA, and may relate to clinical manifestations of RA.**

KEY WORDS: Rheumatoid arthritis, Osteoarthritis, Rheumatoid factor, Autoantibody, PGSF1a, Pituitary, RF-negative RA, Seronegative RA.

Rheumatoid arthritis (RA) is the most common disabling autoimmune disease affecting 1% of the population. While there has been progress in defining its aetiology and pathogenesis, these are still incompletely understood.

Pituitary gland specific factor 1a (PGSF1a), which was recently identified in our laboratory, is specifically transcribed in the human pituitary gland [1]. Autoantibodies against tissue-specific proteins have proved to be useful markers for the diagnosis of autoimmune diseases. Therefore, we searched for antibodies to PGSF1a protein by sensitive radioligand assay [2, 3] to support the diagnosis of lymphocytic hypophysitis. In our investigation of the specificity of this antibody for pituitary diseases [4], we examined it in patients with RA and other autoimmune diseases. Unexpectedly, this antibody was frequently detected in patients with RA.

In the present study, we examined the prevalence of this antibody and examined its relationship to clinical parameters.

Materials and methods

Serum samples

Serum samples were obtained from 46 patients with RA, 20 with osteoarthritis (OA) and 76 with other autoimmune diseases (14 with systemic lupus erythematosus, six with progressive systemic sclerosis, eight with mixed connective tissue disease, 10 with Hashimoto's thyroiditis, 10 with Graves' disease, 13

Department of Laboratory Medicine (D2) and [1]Department of Orthopaedic Surgery, Osaka University Graduate School of Medicine, Osaka, Japan.

Submitted 3 June 2002; revised version accepted 5 August 2002.

Correspondence to: K. Tatsumi, Department of Laboratory Medicine, Osaka University Graduate School of Medicine (D2), Suita-shi Yamadaoka 2-2, Osaka 565-0871, Japan. E-mail: tatsumi@labo.med.osaka-u.ac.jp

with autoimmune hepatitis and 15 with other autoimmune diseases) as well as 36 healthy controls. All RA patients satisfied the 1987 revised diagnostic criteria of the American College of Rheumatology (formerly, the American Rheumatism Association) [5]. Disease activity was classified as the least erosive disease, more erosive disease and mutilating disease, as reported [6]. OA was diagnosed according to the American College of Rheumatology criteria for the classification of OA of the knee [7]. None of the OA patients had any relevant immunological background or history of systemic inflammation. Rheumatoid factor (RF) was measured by nephelometry, and values less than 15.0 IU/ml were considered to be negative. We obtained informed consent from all patients. In all healthy subjects, six kinds of autoantibodies (antinuclear antibody, anti-DNA antibody, RF, anti-mitochondrial antibody, anti-thyroid microsomal antibody and anti-thyroglobulin antibody) were measured as previously described [8], and subjects who had one or more positive antibodies were strictly excluded so as not to include subclinical autoimmune disease. The mean ages of the patient groups were not significantly different from that of the healthy controls, except for those with OA.

Recombinant ^{35}S-labelled PGSF1a

PGSF1a cDNAs were amplified by polymerase chain reaction (PCR) using the human pituitary cDNA, KOD -plus- (TOYOBO, Osaka, Japan) and the following primers to introduce the *Eco*RI site preceding the initiator ATG and *Xho*I site after the stop codon: 5'-AGAATTCATGCCGGGAATGAGGCTGGTTTG-3' and 5'-TCTCGAGACATTGTTTCTGCCCTCACGGA-3' (*Eco*RI and *Xho*I sites are underlined). After amplification, the PGSF1a cDNAs were digested with *Eco*RI and *Xho*I and cloned into the pET28a (+) expression vector (Novagen, Madison, WI). The resulting PGSF1a *in vitro* transcription vector, pET/PGSF1a, was transcribed and translated *in vitro* using the TNT coupled reticulocyte lysate system (Promega, Madison, WI) according to the manufacturer's instructions. In brief, 1 μg of pET/PGSF1a was incubated at 30°C for 90 min in 100 μl of TNT coupled reticulocyte lysate system mixture and 2 μl L-[^{35}S]methionine (15 mCi/ml) (Amersham Pharmacia Biotech, Tokyo, Japan). The translation products were run on a Nick chromatography column (Amersham Pharmacia Biotech) to remove free ^{35}S-methionine, analysed by sodium dodecyl sulphate polyacrylamide gel electrophoresis (SDS–PAGE) (15% polyacrylamide gel) and autoradiography demonstrated the presence of a 16-kDa band component for PGSF1a. The synthesized ^{35}S-labelled PGSF1a was diluted to 20 000 counts per minute (c.p.m.)/20 μl reaction buffer (NaCl 150 mmol/l, Tris 50 mmol/l, pH 7.4, Tween-20 1 ml/l, bovine serum albumin 4 g/l and NaN_3 1 g/l) and was stored at −80°C until use.

Radioligand assay

Four microlitres of serum and 20 000 c.p.m. ^{35}S-labelled PGSF1a were incubated at 4°C overnight in 50 μl of reaction buffer. After incubation, the reaction mixture was transferred into 96-well filtration plates (Multiscreen HVPP, 0.45 μm, Millipore Corp., Bedford, MA) and precipitated with Protein G-Sepharose 4 Fast Flow (Amersham Pharmacia Biotech) that had been blocked with blocking buffer (150 mmol/l NaCl, 50 mmol/l Tris, pH 7.4, 1 ml/l Tween-20, 30 g/l bovine serum albumin and 1 g/l NaN_3) for 1 h at 4°C. The complexes were washed 10 times with washing buffer (NaCl 150 mmol/l, Tris 50 mmol/l, pH 7.4, Tween-20 10 ml/l) using a 96-well filtration system (Millipore Corp.). The plates were then dried, and OptiPhase SuperMix (PerkinElmer Life Science, Boston, MA, USA) was added to each well. The quantity of precipitated, ^{35}S-labelled PGSF1a was determined using a 1450 MicroBeta TriLux apparatus (PerkinElmer Life Science). All samples were assayed in duplicate. The results obtained from this assay are presented as an anti-PGSF1a antibody index:c.p.m. of the unknown serum/c.p.m. of normal pooled serum. The intra- and interassay variations ranged between 7.3 and 10.9%.

Recombinant human PGSF1a (rhPGSF1a)

Escherichia coli B834 strain BL21 (DE3) was transformed by the pET/PGSF1a. The inclusion body containing rhPGSF1a was purified using BugBuster Protein Extraction Reagent (Novagen) according to the manufacturer's instructions. The inclusion body was resuspended in phosphate-buffered saline (PBS) containing 8 M urea, and rhPGSF1a was purified using TALON Metal Affinity Resins (CLONTECH Laboratories, Inc., Palo Alto, CA) according to the manufacturer's instructions.

Inhibition experiment

An inhibition study with rhPGSF1a or ovalbumin was carried out to confirm the specificity of the antibody by radioligand assay. Serum and ^{35}S-labelled PGSF1a were incubated with or without 1 μg rhPGSF1a or ovalbumin in reaction buffer with 0.16 M urea, and the radioligand assay was carried out as described above.

Immunoblotting analysis

An aliquot of 100 ng of rhPGSF1a was electrophoresed through denaturing 15% acrylamide gel, and was transferred to Hybond-P (Amersham Pharmacia Biotech). After blocking with skimmed milk, the membranes were incubated with sera, which were preincubated with strips of Hybond-P impregnated with 50 μg of rhPGSF1a or bovine serum albumin as a control, for 60 min at room temperature (RT). After washing three times for 10 min with Tris-buffered saline (TBS) (500 mmol/l NaCl, 20 mmol/l Tris, pH 7.4)-0.05% Tween-20 (TBST), the membranes were incubated with a 1:5000 dilution of HRP-Labelled Protein A (Amersham Pharmacia Biotech) in 5% skimmed milk/TBST for 60 min at RT. Subsequently, the proteins were visualized with TMB Membrane Peroxidase Substrate (Kirkegaard & Perry Laboratories, Gaithersburg, MD).

Statistical analysis

The Mann–Whitney U-test was used to compare the anti-PGSF1a antibody indices between the patient groups and the healthy controls. Spearman's correlation coefficient test was used to analyse the relationship among the anti-PGSF1a antibody index, the activity of RF (IU/ml) and C-reactive protein (CRP) concentration (mg/dl) in the patients with RA. A $P < 0.05$ was considered to be significant.

Results

Validation of the radioligand assay

Sera obtained from three patients with RA were diluted in reaction buffer. The dilution curve was linear in the dilution range between 6.25- and 50-fold (data not shown). We therefore decided to use a 1:12.5 dilution in the subsequent experiments.

Specificity and prevalence of autoantibodies against PGSF1a

To confirm the specificity of the radioligand assay, an inhibition study with rhPGSF1a was performed.

The anti-PGSF1a antibody index was decreased when incubated with rhPGSF1a, and was unchanged when incubated with ovalbumin (data not shown). Using an immunoblotting method, anti-PGSF1a antibody was detected, and the signal was absorbed when the serum was preincubated with rhPGSF1a (data not shown).

Using a radioligand assay, we examined sera obtained from patients with various autoimmune diseases and compared them with that from healthy controls (Fig. 1). The mean anti-PGSF1a antibody index was significantly higher in patients with RA ($P < 0.001$) than in healthy controls. With a cut-off value above 1.29 (mean + 2 S.D. of healthy controls), the specificity was 100% and the sensitivities were 43.5% (20/46), 10.0% (2/20) and 5.2% (4/76) for patients with RA, OA and other autoimmune diseases, respectively.

Correlation between anti-PGSF1a antibody and disease activity in RA

When RA patients were divided into three subgroups according to the classification of Ochi *et al.* [6], the mean antibody index in patients with more erosive disease was higher than that in patients with the least erosive disease (Fig. 1).

Relationship among anti-PGSF1a antibody, RF and CRP

No correlation was found between anti-PGSF1a antibody indices and RF titres or CRP concentrations (data not shown), but RF did correlate with CRP ($r = 0.313$, $P < 0.05$). Interestingly, four of eight patients with RF-negative RA had positive anti-PGSF1a antibodies (data not shown).

Discussion

We identified PGSF1a protein as a novel autoantigen in the patients with RA. Although its function is unknown and the amino acid sequence of PGSF1a protein has no homology with other mammalian proteins, it has a weak homology with the soybean nodulin 26B-carboxy terminal domain [1]. It has one sequence (EKRTA) similar

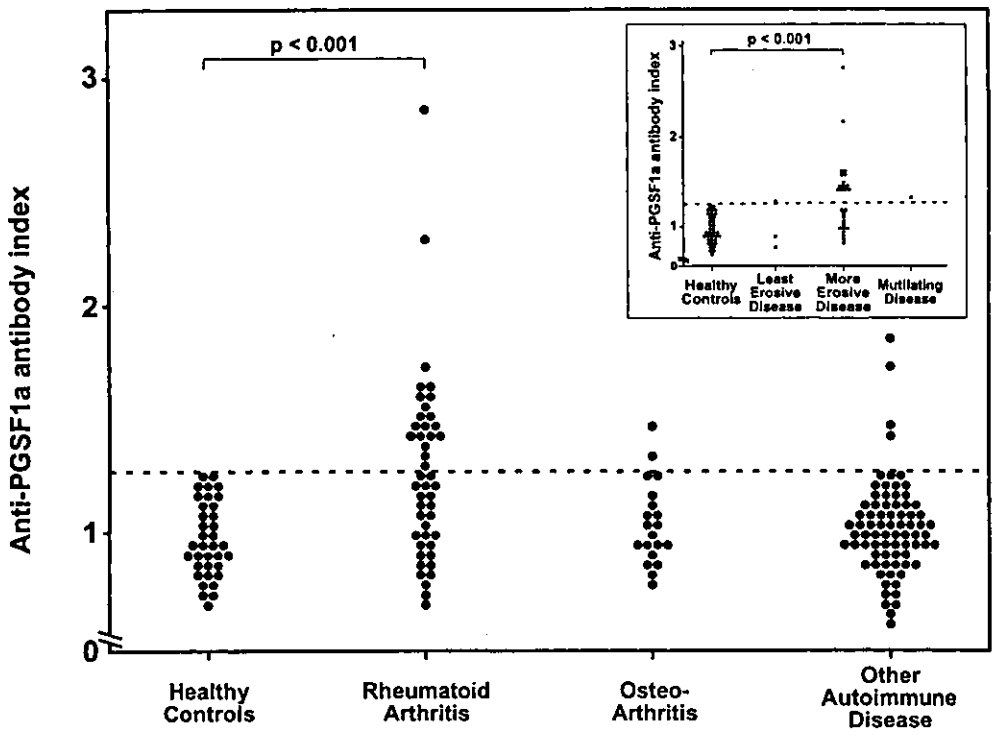

FIG. 1. Anti-PGSF1a indices in control subjects, patients with RA, OA and other autoimmune diseases by radioligand assay. The horizontal dotted line indicates the cut-off value (1.29; mean + 2 S.D. of healthy controls). (inset) The distribution of anti-PGSF1a indices in control subjects, and three subgroups of patients with RA according to the classification of Ochi *et al.* [6].

```
PGSF1a                (33)   SRADCLGAPNIRTAPLGRSEKRTAICFS   (61)
                             ||  | |             |||||
HLA-DR-beta-1*0405    (58)   SQKDLLE-----------QRRAAV---   (70)
```

FIG. 2. Sequence homology between PGSF1a and the RA severity-associated 'shared epitope' of HLA-DR molecules. Amino acids for PGSF1a $_{33-61}$ and HLA-DR-beta-1*0405 $_{58-70}$ are indicated. The identical and conserved amino acids are indicated by bold and underlined type, respectively.

to the RA severity-associated 'shared epitope' sequence of HLA-DR (QK/RRAA) molecules [9, 10] (Fig. 2). Patients with a double dose of the shared sequence tend to have more serious disease manifestations. Thus it may be speculated that the presence of anti-PGSF1a antibodies has a casual relationship to RA.

The measurement of RF is one of the most useful serological tests for the diagnosis of RA, but approximately 20% of patients have RF-negative RA. In the present study, anti-PGSF1a antibody indices did not correlate with RF or CRP, and 50.0% of RF-negative RA patients had positive anti-PGSF1a antibodies. As anti-PGSF1a antibodies were independent of RF, the measurement of anti-PGSF1a antibody will support the diagnosis of RA in RF-negative RA patients.

It is of interest whether the anti-PGSF1a antibodies modify the clinical features of RA. The presence of the anti-PGSF1a antibodies appeared to be linked to severe manifestations of RA, i.e. more erosive disease and mutilating disease conditions [11] (Fig. 1). Therefore it may be important to examine the relationship between disease progress and antibody activity.

Because PGSF1a is a pituitary-specific protein, the relationship between RA and pituitary dysfunction may be interesting to pursue. In patients with RA, a number of studies have shown inappropriate cortisol and sex hormone production [12]. However, little is known regarding pituitary dysfunction in RA. In newly diagnosed and untreated patients with RA, growth hormone response to growth hormone-releasing hormone is disturbed [13]. As anti-PGSF1a antibodies were found in patients with pituitary disorders in our recent study [4] and were found frequently in patients with RA in this study. Anti-PGSF1a antibodies might play a role in pituitary dysfunction among patients with RA and may be a possible risk factor for pituitary dysfunction among patients with RA.

In conclusion, anti-PGSF1a antibody is a useful marker for diagnosis of RA and may relate to clinical manifestations of RA.

Acknowledgements

This work was supported in part by grants from the Ministry of Education, Culture, Sports, Science and Technology; the Ministry of Health, Labour and Welfare of Japan.

References

1. Tanaka S, Tatsumi K, Okubo K *et al.* Expression profile of active genes in the human pituitary gland. J Mol Endocrinol 2002;28:33–44.
2. Grubin CE, Daniels T, Toivola B *et al.* A novel radioligand binding assay to determine diagnostic accuracy of isoform-specific glutamic acid decarboxylase antibodies in childhood IDDM. Diabetologia 1994;37:344–50.
3. Petersen JS, Hejnaes KR, Moody A *et al.* Detection of GAD65 antibodies in diabetes and other autoimmune diseases using a simple radioligand assay. Diabetes 1994;43:459–67.
4. Tanaka S, Tatsumi K, Kimura M *et al.* Detection of autoantibodies against the pituitary-specific proteins in patients with lymphocytic hypophysitis. Eur J Endocrinol 2002;147:767–75.
5. Arnett FC, Edworthy SM, Bloch DA *et al.* The American Rheumatism Association 1987 revised criteria for the classification of rheumatoid arthritis. Arthritis Rheum 1988;31:315–24.
6. Ochi T, Iwase R, Yonemasu K *et al.* Natural course of joint destruction and fluctuation of serum C1q levels in patients with rheumatoid arthritis. Arthritis Rheum 1988; 31:37–43.
7. Altman R, Asch E, Bloch D *et al.* Development of criteria for the classification and reporting of osteoarthritis. Classification of osteoarthritis of the knee. Diagnostic and Therapeutic Criteria Committee of the American Rheumatism Association. Arthritis Rheum 1986;29:1039–49.
8. Iijima T, Tada H, Yagoro A *et al.* Incidence of postpartum onset of disease among patients with rheumatoid arthritis. J Rheumatol 1999;26:755–6.
9. Wakitani S, Murata N, Toda Y *et al.* The relationship between HLA-DRB1 alleles and disease subsets of rheumatoid arthritis in Japanese. Br J Rheumatol 1997; 36:630–6.
10. Weyand CM, Goronzy JJ. The molecular basis of rheumatoid arthritis. J Mol Med 1997;75:772–85.
11. Tomita T, Shimaoka Y, Kashiwagi N *et al.* Enhanced expression of CD14 antigen on myeloid lineage cells derived from the bone marrow of patients with severe rheumatoid arthritis. J Rheumatol 1997;24:465–9.
12. Straub RH, Cutolo M. Involvement of the hypothalamic–pituitary-adrenal/gonadal axis and the peripheral nervous system in rheumatoid arthritis: viewpoint based on a systemic pathogenetic role. Arthritis Rheum 2001; 44:493–507.
13. Templ E, Koeller M, Riedl M *et al.* Anterior pituitary function in patients with newly diagnosed rheumatoid arthritis. Br J Rheumatol 1996;35:350–6.

OsteoArthritis and Cartilage (2003) 11, 278–284

doi:10.1016/S1063-4584(03)00004-9

Osteoarthritis and Cartilage

ICRS International Cartilage Repair Society

OARSI OSTEOARTHRITIS

Localization of bone morphogenetic protein-2 in human osteoarthritic cartilage and osteophyte

T. Nakase M.D., Ph.D.†‡*, T. Miyaji M.D.‡, T. Tomita M.D., Ph.D.‡, M. Kaneko M.D., Ph.D.§, K. Kuriyama M.D.‡, A. Myoui M.D., Ph.D.‡, K. Sugamoto M.D., Ph.D.‡‖, T. Ochi M.D., Ph.D.‖ and H. Yoshikawa M.D., Ph.D.‡

† *Department of Orthopaedic Surgery, Osaka National Hospital, Osaka, Japan*
‡ *Department of Orthopaedic Surgery, Osaka University Graduate School of Medicine, Suita, Japan*
§ *Department of Orthopaedic Surgery, Osaka Chuou Hospital, Osaka, Japan*
‖ *Department of Computer Integrated Medicine, Osaka University Graduate School of Medicine, Suita, Japan*

Summary

Objectives: To examine the localization of bone morphogenetic protein (BMP)-2 mRNA and protein in human osteoarthritic (OA) articular cartilage and osteophyte.

Design: Five normal, four growing and 14 OA human cartilage samples, graded histomorphologically by Mankin Score, were studied by *in situ* hybridization and immunohistochemistry for the expression of BMP-2.

Results: BMP-2 mRNA was present in chondrocytes in neonatal growing articular cartilage, but was scarcely present in normal adult articular cartilage. In OA articular cartilage, BMP-2 mRNA and protein were detected in both clustering and individual chondrocytes in moderately or severely damaged OA cartilage. In moderately damaged OA cartilage, BMP-2 mRNA was localized in both upper and middle zone chondrocytes, but was not detected in deep layer chondrocytes. In severely damaged OA cartilage, cellular localization of BMP-2 mRNA was extended to the deep zone. In the area of osteophyte formation, BMP-2 mRNA was intensely localized in fibroblastic mesenchymal cells, fibrochondrocytes, chondrocytes and osteoblasts in newly formed osteophytic tissue. The pattern of BMP-2/4 immunolocalization was associated with that of mRNA localization.

Conclusions: BMP-2 mRNA and BMP-2/4 were detected in cells appearing in OA tissues. BMP-2 was localized in cells of degenerating cartilage as well as osteophytic tissue. Given the negative localization of BMP-2 in normal adult articular cartilage, BMP-2 might be involved in the regenerating and anabolic activities of OA cells, which respond to cartilage damage occurring in osteoarthritis.

Key words: Osteoarthritis, Bone morphogenetic protein, Osteophyte.

Introduction

Osteoarthritic (OA) change in cartilage is characterized by loss of matrix molecules including proteoglycans and collagen[1,2]. However, the cells that appear during these degenerative events are thought to have anabolic actions, such as proliferation and synthesis of cartilage matrix components[1–3]. These cells also reportedly regain the chondrogenic phenotype and are committed to the regenerative pathway, based on the results that Col IIA, a marker for chondroprogenitor cells, has been reexpressed in OA cells[4].

Various factors may potentiate and regulate this regenerating action of OA cells. One of the potent chondrogenic factors, transforming growth factor-β (TGF-β), was reported to play a role in the process of osteophyte formation in animal models[5,6] and is expressed in human OA cartilage[7]. Bone morphogenetic protein (BMP) is a member of the TGF-β superfamily, and is a strong bone/cartilage inductive molecule *in vivo* and *in vitro*[8,9]. Previous immunohistochemical and *in situ* hybridization studies clarified that BMP is induced and localized in cells under various osteochondrogenic conditions, suggesting the involvement of BMP in osteo/chondro inductive events *in vivo*[9,10]. Furthermore, we recently reported that several BMP genes are localized at the site of chondrogenesis in a mice spondylosis model that histologically resembles the degenerative process of cartilage in humans[11]. To date, almost 30 members of the BMP family have been identified[9], and among its members, BMP-2 has the capacity to induce osteochondrogenesis[3,9], and reportedly promotes growth and matrix synthesis of chondrocytes[5,12]. This chondrogenic action of BMP-2 easily leads us to question the involvement and role of this molecule in OA. However, to date, there have been no reports of the expression and localization of BMP-2 in OA tissue.

The purpose of this study was to elucidate the localization of BMP-2 mRNA and protein in surgical OA specimens and in normal cartilage using immunohistochemistry and *in situ* hybridization.

*Address correspondence and reprint requests to: Dr Takanobu Nakase, Department of Orthopaedic Surgery, Osaka National Hospital, 2-1-14, Houenzaka, Chuou-ku, Osaka 540-0006, Japan. Tel: 81-6-6942-1331; Fax: 81-6-6943-6467; E-mail: nakase@onh.go.jp

Received 26 August 2002; revision accepted 24 December 2002.

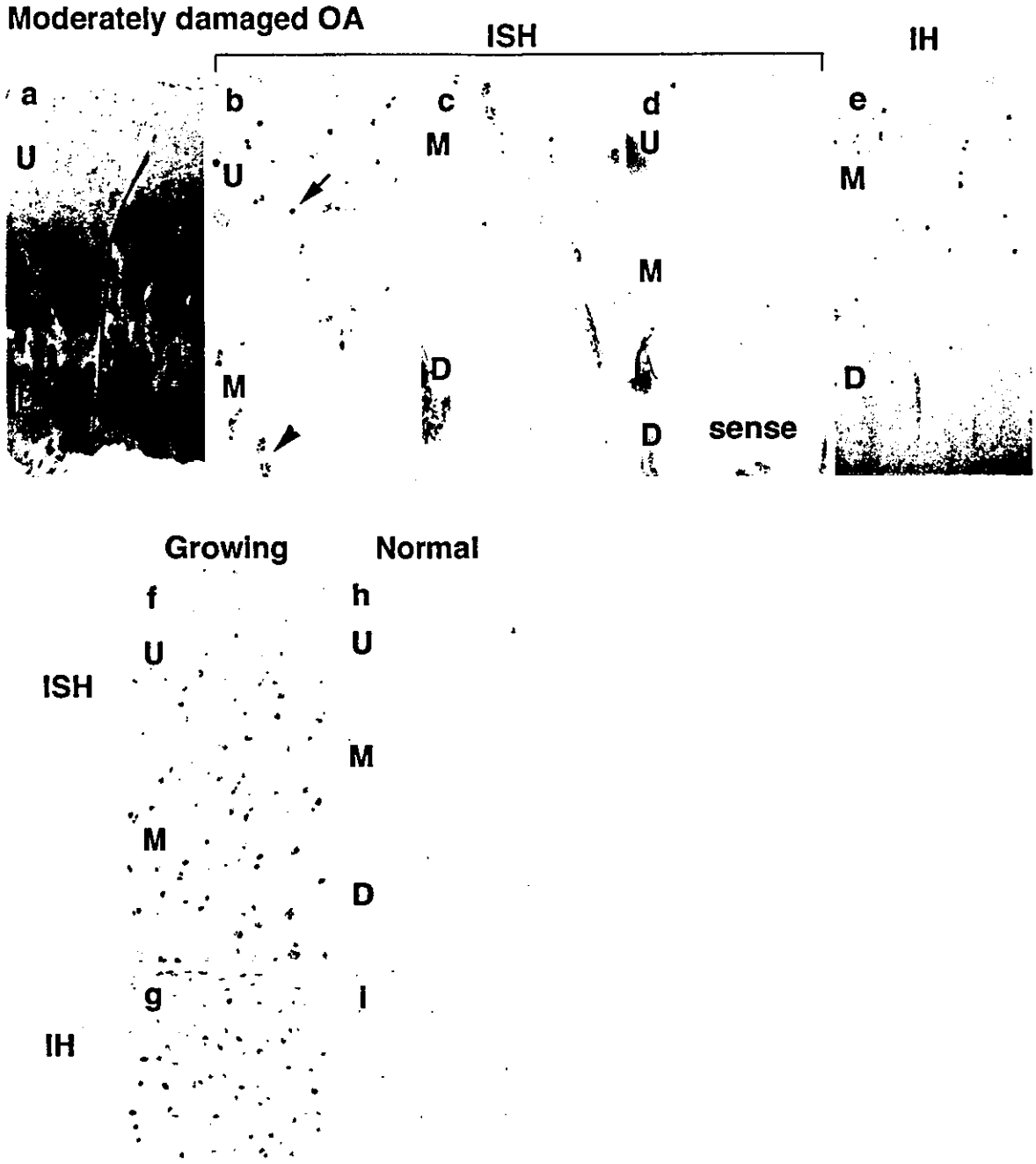

Fig. 1. Histological sections of moderately damaged OA (a–e; Mankin grade 3), growing (f, g) and normal articular cartilage (h, i). Safranin-O/fast green staining (a); *in situ* hybridization (ISH) with antisense (b, c, f, h) and with sense (d) human BMP-2 cRNA probe; and immunohistochemistry (IH) with anti-BMP-2/4 antibody (e, g, i). (U, upper zone; M, middle zone; D, deep zone; growing, growing neonatal cartilage; normal, normal adult cartilage) (a) Safranin-O staining was decreased in the upper layer, but preserved in the middle and deep layers. (b, c) BMP-2 mRNA was detected in individual (arrow) and clustering (arrow head) chondrocytes in the upper and middle layers (b). In contrast, BMP-2 mRNA was not detected in deep zone cells (c). (d) No signals were detected with sense probe (continuous section from a). (e) BMP-2/4 was immunolocalized in chondrocytes in the middle zone (M). In contrast, immunoreactivity was not apparent in deep zone (D) chondrocytes. (f, g) BMP-2 transcripts (f) and positive immunostaining for BMP-2/4 (g) were observed in articular chondrocytes in human neonatal growing articular cartilage (ankle joint). (h, i) BMP-2 transcripts (h) and positive immunostaining for BMP-2/4 (i) were not detected in cells in normal adult articular cartilage (knee joint). Original magnification: ×40 (a, d, f, h); ×100 (b, c, e); and ×200 (g, i).

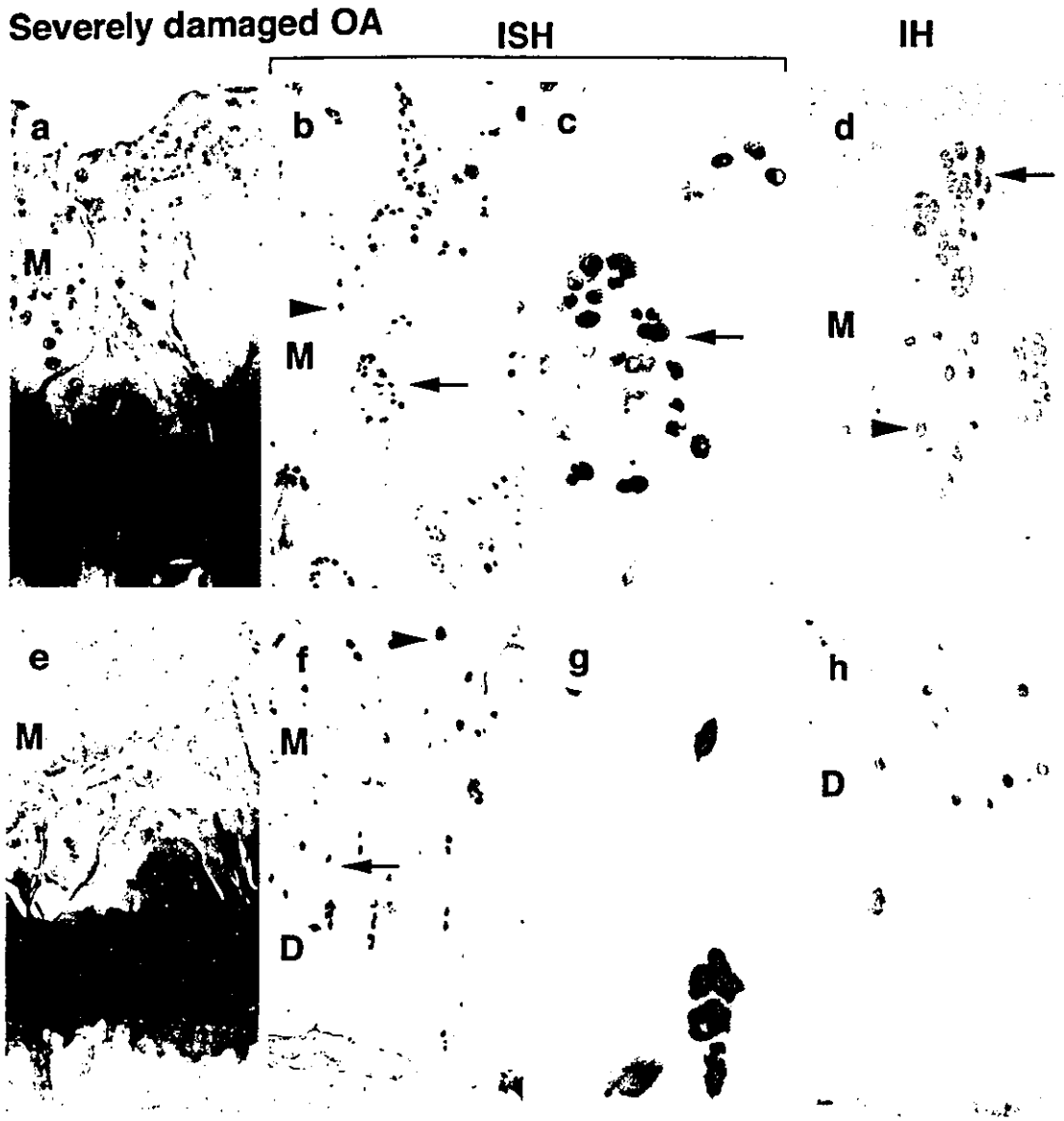

Fig. 2. Histological sections of severely damaged OA cartilage (Mankin grade 9). Staining of safranin-O/fast green (a, e); *in situ* hybridization (ISH) with antisense human BMP-2 cRNA probe (b, c, f, g); and immunohistochemistry (IH) with anti-BMP-2/4 antibody (d, h). (U, upper zone; M, middle zone; D, deep zone) (a) Upper zone was essentially lost and staining for safranin-O was lacking in the middle zone. (b) Intense signals for BMP-2 transcripts were detected in both individual (arrow head) and clustering chondrocytes (arrows) in the middle layer in which the territorial matrix was less stained by safranin-O. (c) Higher magnification of arrow area in (b) in the middle zone. BMP-2 mRNA was detected in clustering chondrocytes. (d) Positive immunostaining for BMP-2/4 was detected both in the individual (arrow head) and clustering (arrow) chondrocytes in the middle layer (nearby section to a). (e) Upper zone was essentially lost and positive staining for safranin-O was apparent in the territorial matrix of the deep zone chondrocytes. (f) BMP-2 mRNA was localized in middle layer chondrocytes (arrow head). BMP-2 mRNA was also detected in both individual and clustering chondrocytes in the deep layer (arrow), whose territorial matrix was stained by safranin-O. (g) Higher magnification of arrow area in (f). BMP-2 mRNA was detected the deep layer chondrocytes. (h) BMP-2/4 was also immunolocalized in deep layer chondrocytes. Original magnification: ×40 (a, e); ×100 (b, f); ×200 (d, h); and ×400 (c, g).

Materials and methods

TISSUE SAMPLING AND PREPARATION

Cartilage specimens with subchondral bone were obtained from 10 female and four male patients (age range, 65 to 75 years) undergoing endoprosthetic surgery for OA of the knee joints (medial and lateral femoral condyles and tibial articular surfaces). All the cases satisfied the American College of Rheumatology classification criteria for OA of the knee[13]. Cases of rheumatoid arthritis were excluded. Five macroscopically normal cartilage specimens with subchondral bone were obtained from five patients undergoing amputation (age range, 36 to 66 years; two medial femoral condyles, two tali of ankle joint and one metatarsal head of interphalangeal joints). In addition, four growing articular cartilage samples were obtained from four patients undergoing amputation (age range, 1 to 4 years; two tali and two metatarsal heads). Written, informed

Table I
Summary of BMP-2 mRNA localization in cells in moderately and severely damaged OA cartilage

Degree of damage	Type of chondrocytes	Zone		
		Upper	Middle	Deep
Moderate	Individual	+~++	+~++	−~±
	Clustering	+~+++	++~+++	−~+
Severe	Individual	*	++~+++	++~+++
	Clustering	*	++~+++	+++

Numbers of individual and clustering chondrocytes positive for BMP-2 mRNA were counted. Ratio indicates positive individual chondrocytes/total individual chondrocytes, and positive clustering chondrocytes/total clustering chondrocytes.
−, 0%; ±, ~10%; +, ~25%; ++, 25–50%; +++, 50–75%.
*Upper zone was almost lost.

consent was obtained from all the patients or legal guardians. Obtained tissues were fixed in 4% paraformaldehyde (Merck KGaA, Darmstadt, Germany) in PBS (pH, 7.4) (Sigma Chemical Co., St. Louis, MO) at 37°C for 24 h, decalcified in 20% EDTA (if needed) and dehydrated in an ethanol series before being embedded in paraffin as described[10,14]. The size of each section ranged from approximately 0.8×1 to 1.5×2.8 cm. Each 5-μm section was made on a microtome, and the sections were stained with safranin-O/fast green to reveal cartilaginous matrix. Three sections from each specimen were used for immunohistochemistry and *in situ* hybridization. The histological samples were graded according to the method of Mankin *et al.*[15].

PREPARATION OF RNA PROBES

cDNA for human BMP-2[16] (encoding the propeptide region relatively specific for BMP-2; with less than 54% homology with human BMP-4 and less than 33% homology with human BMP-6 and BMP-7) was subcloned into a pGEM-T plasmid, and then either linealized by Sac II and transcribed by SP6 RNA polymerase to generate antisense probes or linealized by Spe I and transcribed by T3 RNA polymerase to generate sense probes as described[16]. Northern blotting experiments using ^{32}P-labeled antisense transcripts and the human osteosarcoma cell line showed a specific band (data not shown). The antisense probe for 18S ribosomal RNA (rRNA) was prepared as described[3] and was used to confirm the preservation of RNA in the tissue specimens.

IN SITU HYBRIDIZATION

In situ hybridization was performed as previously described[10,16]. Briefly, paraffin-embedded sections were dewaxed, rehydrated, and fixed with 4% paraformaldehyde for 20 min. The sections were then treated with 0.2 N HCl for 10 min to inactivate endogenous alkaline phosphatase, and were acetylated with 0.25% acetic anhydride in 0.1 M triethanolamine (pH, 8.0) for 10 min. They were then dehydrated with an ethanol series and were air-dried. Each section was covered by 50 μl of hybridization solution (50% formamide, 10% dextran sulfate, 1×Denhardt's solution, 600 mM NaCl, 0.25% SDS, 150 μg/ml of *Escherichia coli* tRNA, approximately 0.5 μg/ml of RNA probe) and incubated at 50°C for 16 h. After hybridization, the slides were briefly washed in 5×SSC (1×SSC=0.15 M NaCl, 0.015 M sodium citrate) and in 50% formamide, 2×SSC for 30 min at 50°C. RNase A treatment (10 μg/ml) proceeded at 37°C for 30 min. The slides were washed twice with 2×SSC and 0.2×SSC for 20 min at 50°C. Hybridized probes were detected using a Nucleic Acid Detection Kit (Boehringer Mannheim GmbH Biochemica, Mannheim, FRG) according to the manufacturer's instructions.

Controls included: (i) hybridization with the sense (mRNA) probe, (ii) RNAse A treatment (20 μg/ml) prior to hybridization, and (iii) use of neither antisense nor anti-digoxigenin antibody. The three controls showed no positive signals. The cell count assessment for positive cells was done at ×200 magnification using a NIKON ECRIPS E800M microscope (Nikon, Tokyo, Japan) as described[11].

IMMUNOHISTOCHEMISTRY

Immunohistochemistry was performed using the streptoavidin–peroxidase method with histofine SAB-PO kits (Nichirei, Tokyo, Japan) as described with minor modification[12]. A mouse monoclonal antibody against human BMP-2/4 (h3b2/17.8.1, kindly donated by Genetics Institute, Inc., MA)[14,15] was used as a primary antibody at a concentration of 10 μg/ml. Among several BMP members (BMPs 1 to 7), only BMP-2 and -4 were found to react with this antibody by immunoblotting with purified recombinant proteins[17]. Tissue sections were briefly deparaffinized and were incubated with 2 mg/ml hyaluronidase in phosphate buffered saline (PBS; pH, 7.5) for 20 min. The sections were digested with 1 mg/ml pronase (Boehringer Mannheim GmbH Biochemica, Mannheim, FRG) in PBS (pH, 7.5) and placed in 3% H_2O_2 in methanol for 30 min to block endogenous peroxidase. After washing in PBS, the sections were blocked with 10% normal serum of the same species as the secondary antibody to minimize background staining, before being incubated with primary antibody for 2 h at room temperature. Normal serum of the same species as the primary antibody was used as a control for the primary antibody. After washing in PBS, the sections were incubated with secondary antibody at a concentration of 1:100 (rabbit anti-mouse Ig-G: Nichirei) for 20 min at room temperature in a humid chamber, and then incubated with peroxidase-conjugated streptoavidin (Nichirei), again for 20 min at room temperature in a humid chamber and washed in PBS. Finally, color reaction was performed using the substrate reagent 3,3'diaminobenzidine tetrahydrochloride (DAB) (Dojindo, Tokyo, Japan). This final solution contained 120 ml of Tris–HCl (pH, 7.6), 15 mg of DAB and 6.8 μl of 35% H_2O_2. Sections were counterstained with hematoxylin and mounted. As a control for immunostaining, normal serum from the same species as the primary antibody (mouse-Ig-G) was used.

Results

BMP-2 LOCALIZATION IN OA CARTILAGE

In situ hybridization detected BMP-2 mRNA in cells at various Mankin grades in OA cartilage (Figs. 1 and 2). BMP-2 mRNAs were localized in both clustering and individual chondrocytes.

In moderately damaged OA cartilage (Mankin grade 3–6; Fig. 1), staining of safranin-O was still preserved in the middle and deep layers [Fig. 1(a)]. BMP-2 mRNA was localized in chondrocytes in both the upper and middle layers [Fig. 1(b)]. In contrast, BMP-2 transcript was

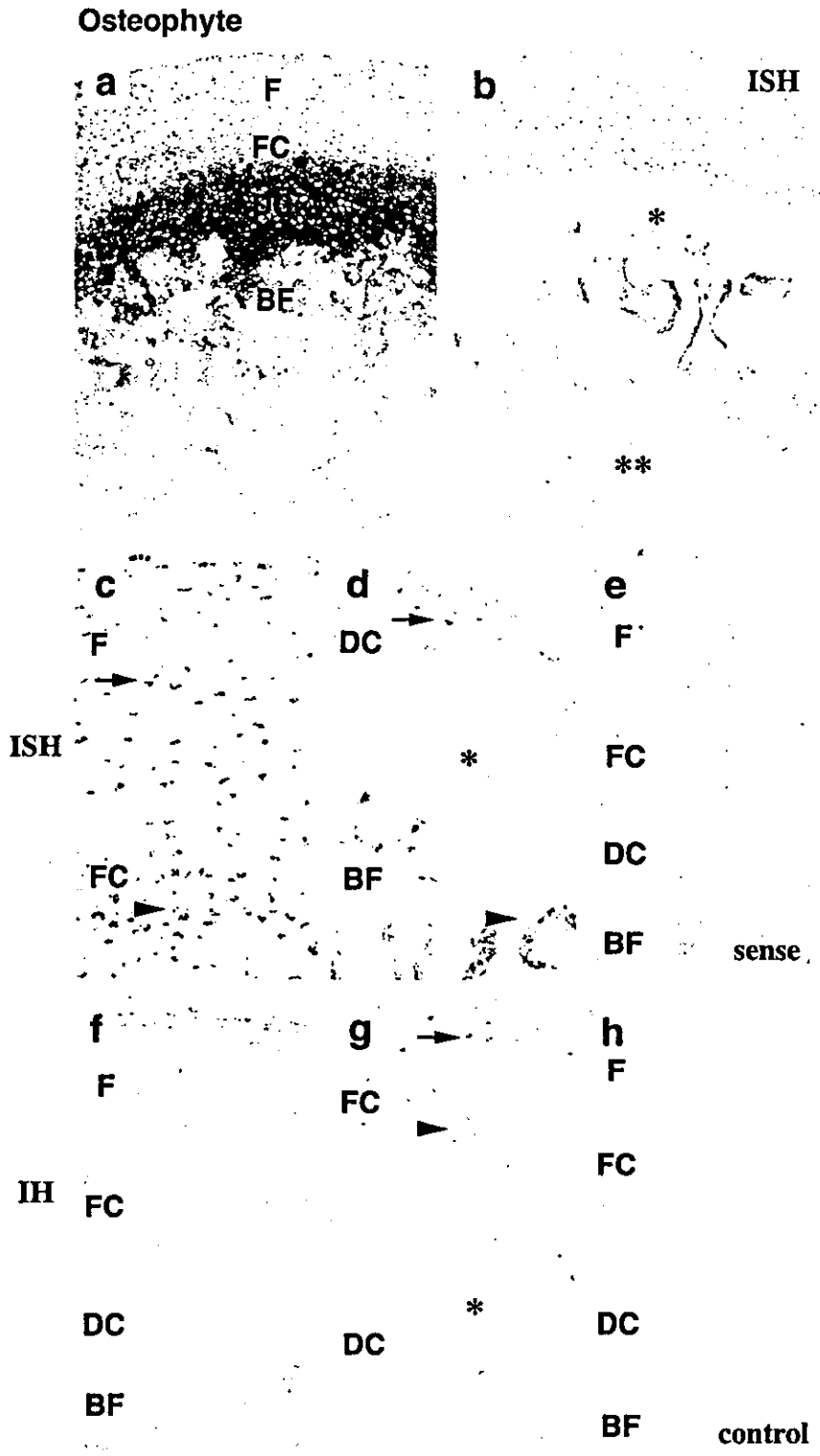
Osteophyte
a
F
FC
BE
b
ISH
*
**
c
d
e
F
DC
F
ISH
*
FC
DC
FC
BF
BF
sense
f
g
h
F
F
FC
FC
IH
FC
*
DC
DC
DC
BF
BF
control

scarcely detected in deep layer chondrocytes [Fig. 1(c)], although these cells were positive for 18S rRNA (data not shown). No signals were detected with BMP-2 sense probe [Fig. 1(d)]. BMP-2/4 was immunolocalized in the upper layer (data not shown) and middle layer chondrocytes, but was scarcely immunolocalized in deep layer chondrocytes [Fig. 1(e)].

BMP-2 mRNA and BMP-2/4 were localized in neonatal growing articular chondrocytes [Fig. 1(f,g)]. In contrast, BMP-2 mRNA was absent and BMP-2/4 was not localized in normal adult cartilage cells [Fig. 1(h,i)].

In severely damaged OA cartilage (Mankin grade 7–12; Fig. 2), staining intensity of safranin-O noticeably decreased. BMP-2 transcripts were detected not only in middle zone chondrocytes [Fig. 2(a–c)], but also in deep zone chondrocytes [Fig. 2(e–g)]. In the middle layer, BMP-2 transcripts were located in clustering chondrocytes whose territorial matrix lacked safranin-O staining [Fig. 2(a–c)]. In the deep layer, BMP-2 mRNA was localized in chondrocytes whose territorial matrix was stained with safranin-O [Fig. 2(e–g)]. BMP-2/4 was immunolocalized both in the middle and deep layer chondrocytes [Fig. 2(d,h)], and was immunolocalized in both individual and clustering chondrocytes [Fig. 2(d,h)].

The pattern of BMP-2 mRNA localization in OA cartilage is summarized in Table I. The pattern of BMP-2/4 immunolocalization was associated with that of mRNA localization.

BMP-2 LOCALIZATION IN OSTEOPHYTIC TISSUE

BMP-2 mRNA was intensely localized in cells in osteophytic tissue [Fig. 3(a–d)]. BMP-2 transcripts were localized in fibroblastic cells in the outer fibrous layer [Fig. 3(b,c)], in fibrochondrocytes in the fibrocartilage layer [Fig. 3(b,d)] and in osteoblasts in the bone-forming area adjacent to the chondrogenic layer [Fig. 3(b,d)]. The majority of chondrocytes in the deep cartilage layer were positive for BMP-2. However, chondrocytes in the very deep layer close to the bone-forming site showed no, or only faint, signals for BMP-2 transcripts [Fig. 3(b,d)]. BMP-2 transcripts were absent in osteoblasts located in the relatively mature bone at the center of the osteophyte [Fig. 3(b)]. No signals were detected with the BMP-2 sense probe [Fig. 3(e)]. BMP-2/4 immunolocalization was associated with mRNA localization [Fig. 3(f,g)]. Negative control using normal mouse serum showed no staining [Fig. 3(h)].

Discussion

To the best of our knowledge, this is the first report to describe the localization of BMP-2 in human OA tissues. BMP-2 was scarcely detected in adult normal cartilage, but was notably present in the OA cells. These findings indicate the possible synthesis of BMP-2 by OA cells and involvement of BMP-2 in the OA state. BMP-2 was synthesized by both individual and clustering chondrocytes. Even deep zone chondrocytes synthesized BMP-2 in severe OA cartilage, where cartilage damage was extended to the deeper area, although these cells did not synthesize BMP-2 when cartilage damage was less significant. These findings suggest that the zone-specific distribution of BMP-2 may be dependent on the degree of OA damage.

Our findings of this study, as well as those of previous reports[3,18], indicate that some of the BMP-2 positive cells are associated with proteoglycan synthesis, as evident by positive staining for safranin-O in the territorial matrix. This tendency was particularly marked in the lower middle and deep layers. OA chondrocytes in the middle and deep layers reportedly synthesize several cartilaginous collagens[3] and aggrecan mRNA[18]. Another study has reported that BMP-2 stimulates the synthesis of proteoglycan synthesis in articular cartilage[5]. Given our results and those of previous reports, BMP-2 localization in safranin-O positive areas suggests the possible involvement of BMP-2 in neo-matrix synthesis occurring in OA tissue. We found clustering chondrocytes whose territorial matrix lacked safranin-O staining. These types of cells are thought to be in a proliferating state[2]. BMP-2 was localized in these types of cells and given that BMP-2 reportedly promoted growth of chondrocytes in *in vitro* culture experiments[12], BMP-2 may be involved in OA cell proliferation as well as matrix synthesis.

Significant BMP-2 expression was observed in osteophytic tissue. BMP-2 was detected in the early mesenchymal layers as well as in fibrochondrocytes, suggesting the role of BMP-2 in induction and promotion of osteophyte formation. Such osteochondro-inductive action of BMP-2 has been proposed by previous *in vivo* and *in vitro* studies[8,9]. In the present study, the localization of BMP-2 in OA chondrocytes at various Mankin grades in various zones and in fibrochondrocytes in the osteophyte is somewhat similar to that of Col IIA[4]. As Col IIA is reportedly a marker for chondroprogenitor cells and binds to BMP-2, BMP-2 may be involved in the early chondrogenic events via the BMP-2/Col IIA complex, leading to further matrix synthesis in OA cartilage and osteophyte formation.

As BMP-2/4 could not be detected in the extracellular matrix (ECM) in OA cartilage during the present experiments, but was localized in OA cells, it is possible that the amount of BMP-2/4 in ECM is considerably small, or the lack of BMP-2/4 localization in the ECM might be due to the technical limitations of the sensitivity of our

Fig. 3. (a) Staining of safranin-O/fast green; *in situ* hybridization (ISH) (b–d) with antisense and (e) sense human BMP-2 cRNA probes; and (f, g) immunohistochemistry (IH) with anti-BMP-2/4 antibody and (g) normal mouse serum in histological sections of human osteophytic tissue. (a, b) BMP-2 mRNA was detected in fibroblastic mesenchymal cells in the outer fibrous layer (F), in fibrochondrocytes in the middle fibrocartilage layer (FC) and in chondrocytes in the deep chondrocyte layer (DC). In contrast, BMP-2 transcript was absent in cells in the very deep zone [asterisk in (b)] of the deep cartilage layer close to the bone-forming area. BMP-2 signals were present in osteoblasts in the bone-forming layer (BF), but absent in cells in mature bone located at the center [double asterisks in (b); (a, b, e, f) are nearby sections]. (c) Higher magnification of the F and FC layers shown in (b). Intense signals for BMP-2 mRNA were detected in fibroblastic cells (arrow) and fibrochondrocytes (arrow head). (d) Higher magnification of the DC and the BF layers is presented in (b). BMP-2 transcripts were detected in chondrocytes (arrow) and osteoblasts (arrow head). In contrast, no, or faint, signals for BMP-2 mRNA were detected in the very deep zone chondrocytes (asterisk) close to the BF area. (e) No apparent signals were detected in any layer by human BMP-2 sense probe. Positive BMP-2/4 staining was observed in cells in the outer fibrous (F) layer. (f, g) Positive immunostaining for BMP-2/4 was detected in cells in the outer fibrous layer (F) (f), the middle fibrocartilage layer (FC) (f and arrow in g), and in chondrocytes in the deep chondrocytes layer (DC) (g and arrow head in g). (h) Negative control. No immunostaining was observed with mouse normal serum. Original magnification: ×40 (a, b); ×100 (e, f, h); and ×200 (c, d, g).

immunohistochemical methods. These possibilities should be further investigated. In addition, several other growth factors, such as TGF-β[7] insulin-like growth factor[19], basic fibroblast growth factor[7], hepatocyte growth factor[20], vascular endothelial cell growth factor[21] and cartilage-derived morphogenetic protein-1[22], are reported to be expressed in OA cartilage. BMP-2 may act synergistically with these growth factors or share roles in the metabolism of OA cartilage. A recent publication, in particular, has proved the potent role of TGF-β in osteophyte formation in an experimental animal model[6]. Future studies should aim to elucidate the precise roles of BMP-2 in OA change.

In conclusion, this is the first report to demonstrate BMP-2 localization in OA tissue. The present findings, together with those of previous reports, suggest the anabolic role of OA chondrocytes via synthesis of BMP-2 and the potential capacity of articular chondrocytes to synthesize BMP-2 in response to the cartilage damage that occurs in osteoarthritis.

Acknowledgements

We thank Miss Kaori Izumi and Miss Kanae Asai for their technical assistance for preparing tissue sections. We also thank Forte Technical Scientific and Corporate Communications for editorial assistance.

References

1. Poole AR. An introduction to the pathophysiology of osteoarthritis. Front Biosci 1999;15:D662–70.
2. Hough JAJ. Pathology of osteoarthritis. In: Koopman WJ, Ed. Arthritis and Allied Conditions. A Textbook of Rheumatology 14th edn. Philadelphia, USA: Lippincott, Williams & Wilkins 2001;2167–94.
3. Aigner T, Bertling W, Stoss H, Weseloh G, von der Mark K. Independent expression of fibril-forming collagens I, II, and III in chondrocytes of human osteoarthritic cartilage. J Clin Invest 1993;91:829–37.
4. Aigner T, Zhu Y, Chansky HH, Matsen FA 3rd, Maloney WJ, Sandell LJ. Reexpression of type IIA procollagen by adult articular chondrocytes in osteoarthritic cartilage. Arthritis Rheum 1999; 42:1443–50.
5. van Beuningen HM, Glansbeek HL, van der Kraan PM, van den Berg WB. Differential effects of local application of BMP-2 or TGF-beta 1 on both articular cartilage composition and osteophyte formation. Osteoarthritis Cartilage 1998;6:306–17.
6. Scharstuhl A, Glansbeek HL, van Beuningen HM, Vitters EL, van der Kraan PM, van den Berg WB. Inhibition of endogenous TGF-beta during experimental osteoarthritis prevents osteophyte formation and impairs cartilage repair. J Immunol 2002; 169:507–14.
7. Uchino M, Izumi T, Tominaga T, Wakita R, Minehara H, Sekiguchi M, *et al.* Growth factor expression in the osteophytes of the human femoral head in osteoarthritis. Clin Orthop 2000;377:119–25.
8. Wozney JM, Rosen V, Celeste AJ, Mitsock LM, Whitters MJ, Kriz RW, *et al.* Novel regulators of bone formation: molecular clones and activities. Science 1988;242:1528–34.
9. Kawabata M, Miyazono K. Bone morphogenetic proteins. In: Canalis E, Ed. Skeletal Growth Factors. Philadelphia, USA: Lippincott, Williams & Wilkins 2000.
10. Nakase T, Nomura S, Yoshikawa H, Hashimoto J, Hirota S, Kitamura Y, *et al.* Transient and localized expression of bone morphogenetic protein 4 messenger RNA during fracture healing. J Bone Miner Res 1994;9:651–9.
11. Nakase T, Ariga K, Miyamoto S, Okuda S, Tomita T, Iwasaki M, *et al.* Distribution of genes for bone morphogenetic protein-4, -6, growth differentiation factor-5, and bone morphogenetic protein receptors in the process of experimental spondylosis in mice. J Neurosurg 2001;94:68–75.
12. De Luca F, Barnes KM, Uyeda JA, De-Levi S, Abad V, Palese T, *et al.* Regulation of growth plate chondrogenesis by bone morphogenetic protein-2. Endocrinology 2001;142:430–6.
13. Altman R, Asch E, Bloch D, Bole G, Borenstein D, Brandt K, *et al.* Development of criteria for the classification and reporting of osteoarthritis. Classification of osteoarthritis of the knee. Diagnostic and Therapeutic Criteria Committee of the American Rheumatism Association. Arthritis Rheum 1986;29:1039–49.
14. Nakase T, Kaneko M, Tomita T, Myoui A, Ariga K, Sugamoto K, *et al.* Immunohistochemical detection of cathepsin D, K, and L in the process of endochondral ossification in the human. Histochem Cell Biol 2000; 114:21–7.
15. Mankin HJ, Dorfman H, Lippiello L, Zarins A. Biochemical and metabolic abnormalities in articular cartilage from osteoarthritic human hips. II. Correlation of morphology with biochemical and metabolic data. J Bone Joint Surg Am 1971;53:523–37.
16. Nakase T, Myoui A, Shimada K, Kuriyama K, Joyama S, Miyaji T, *et al.* Involvement of BMP-2 signaling in a cartilage cap in osteochondroma. J Orthop Res 2001; 19:1085–8.
17. Yoshikawa H, Rettig WJ, Lane JM, Takaoka K, Alderman E, Rup B, *et al.* Immunohistochemical detection of bone morphogenetic proteins in bone and soft-tissue sarcomas. Cancer 1994;74:842–7.
18. Aigner T, Vornehm SI, Zeiler G, Dudhia J, von der Mark K, Bayliss MT. Suppression of cartilage matrix gene expression in upper zone chondrocytes of osteoarthritic cartilage. Arthritis Rheum 1997;40:562–9.
19. Middleton J, Arnott N, Walsh S, Beresford J. Osteoblasts and osteoclasts in adult human osteophyte tissue express the mRNAs for insulin-like growth factors I and II and the type 1 IGF receptor. Bone 1995;16:287–93.
20. Pfander D, Cramer T, Weseloh G, Pullig O, Schuppan D, Bauer M, *et al.* Hepatocyte growth factor in human osteoarthritic cartilage. Osteoarthritis Cartilage 1999; 7:548–59.
21. Pfander D, Kortje D, Zimmermann R, Weseloh G, Kirsch T, Gesslein M, *et al.* Vascular endothelial growth factor in articular cartilage of healthy and osteoarthritic human knee joints. Ann Rheum Dis 2001;60:1070–3.
22. Bobacz K, Gruber R, Soleiman A, Graninger WB, Luyten FP, Erlacher L. Cartilage-derived morphogenetic protein-1 and -2 are endogenously expressed in healthy and osteoarthritic human articular chondrocytes and stimulate matrix synthesis. Osteoarthritis Cartilage 2002;10:394–401.

Eur Radiol (2003) 13:1728–1734
DOI 10.1007/s00330-002-1769-4

Masakazu Fujii
Tetsuya Tomita
Katsuyuki Nakanishi
Motoharu Kaneko
Kenji Hayashida
Kazuomi Sugamoto
Takahiro Ochi
Hideki Yoshikawa

The value and limitation of gadopentetate-enhanced magnetic resonance imaging in detecting the condition of anterior cruciate ligament in rheumatoid knee: comparative study with histology

Received: 31 August 2001
Revised: 15 February 2002
Accepted: 1 October 2002
Published online: 6 December 2002

M. Fujii (✉)
Department of Orthopaedic Surgery,
Garacia Hospital,
Aomadani-nishi, Mino, 562–0023 Osaka,
Japan
e-mail: fujiimasakazu46@hotmail.com
Tel.: +81-727-292345
Fax: +81-727-285166

T. Tomita · M. Kaneko · K. Hayashida
K. Sugamoto · T. Ochi · H. Yoshikawa
Department of Orthopaedic Surgery,
Osaka University Graduate School
of Medicine,
2–2 Yamada-oka, Suita, 565–0871 Osaka,
Japan

K. Nakanishi
Department of Radiology,
Osaka University Graduate School
of Medicine,
2–2 Yamada-oka, Suita, 565–0871 Osaka,
Japan

Abstract The aim of this study was to elucidate the utility and limitation of gadopentetate (Gd)-enhanced MRI as a method for evaluating the anterior cruciate ligament (ACL) in the rheumatoid arthritis (RA) knee, using both surgical macro findings and histological findings to ascertain the pathological condition of the affected knee. Thirty-six knees of 25 RA patients were studied in this study. Four imaging protocols were employed: protocol A, T1-weighted and T2-weighted sagittal images; protocol B, T1-weighted sagittal image, after infusion of Gd-DTPA (0.2 mmol/kg, i.v.); protocol C, T1-weighted angled coronal image, parallel to the ACL; and protocol D, T1-weighted angled coronal image, parallel to the ACL, after infusion of Gd-DTPA. Sagittal image was determined as previously described. Angle coronal image was newly determined as coronal image parallel to the ACL. Surgical and MRI findings of the ACL were classified into four types: Type I (normal group) indicated that the thickness of the ACL was almost normal, adequate tension was maintained (surgical findings), and the ACL had thick and a more complex appearance with a homogeneous signal intensity and well-defined borders (MRI findings). Type II (degenerated group): the ACL had degenerated and tension was reduced (surgical findings), and the ACL had thin and a more complex appearance with a less homogeneous signal intensity and less well-defined borders. This appearance was more evident on Type II than Type I (MRI findings). Type III (ruptured group): the parenchyma of the ACL remained but lacked continuity (surgical findings), and the ACL appeared as partial lack of low signal intensity (MRI findings). Type IV (absent group): the parenchyma of the ACL was practically absent (surgical findings), and the ACL appeared as complete lack of signal low signal intensity (MRI findings). The concordance rate between surgical and MRI findings was investigated. Moreover, we investigated the extent to which histological changes of the ACL could be discriminated using MRI. In RA knees, the overall concordance rate between surgical and MRI findings was 41.7% under imaging protocol A. The overall rate improved up to 69.4% under imaging protocol B. But the overall rate dropped to 36.1% under imaging protocol C. The overall rate improved up to 83.3% under imaging protocol D. Especially, significant differences between imaging protocols A and B ($p<0.05$), and imaging protocols C and D ($p<0.01$), with respect to ACL degenerated group, were recognized. But significant differences between imaging protocols A and C, and imaging protocols B and D, with respect to ACL degenerated group, were not recognized. The concor-

dance rate between histological and MRI findings was 41.7% in ACL normal group, and 61.5% in ACL degenerated group. The concordance rate between surgical and MRI findings was 100% in ACL normal group, and 78.9% in ACL degenerated group. There was a significant difference in the concordance rates between histological, surgical, and MRI findings in normal group ($p<0.05$). The results of this study suggested that with Gd-enhanced MRI, the degree of synovial proliferation around the ACL and the degree of degradation of the ACL in the RA knee can be evaluated more accurately than with conventional MRI; however, in RA knees with severe synovial proliferation, it may be difficult to discriminate between the invasive synovium going into the ligament from synovium surrounding the ligament. This may be a limitation of Gd-enhanced MRI at present. In the clinical setting, the present imaging technique does allow the ligament to be evaluated to a certain degree, and may prove useful in the evaluation of temporal changes in the RA knee.

Keywords Magnetic resonance imaging · Anterior cruciate ligament · Rheumatoid knee

Introduction

Rheumatoid arthritis (RA) causes chronic inflammation of synovial joints, and results in progression of joint destruction over time. The afflicted joint is characterized by synovial proliferation, together with destruction of articular cartilage and a loss of trabecular bone. Recently, considerable light has been shed on the pathogenesis and clinicopathological features of joint destruction at the molecular level, but much remains unknown about its clinical management [1, 2]. Degeneration or rupture of the anterior cruciate ligament (ACL) is frequently seen during synovectomy or total knee arthroplasty (TKA) for the RA knee, and in severe cases, this degeneration process may even extend to the posterior cruciate ligament (PCL) [3]; however, the medical literature only includes scattered references to the pathological features of this condition. The ACL plays a key role in stabilizing the knee, and instability caused by the ACL degeneration may have a significant involvement in joint destruction of the knee [4]. Synovectomy is extensively performed as a treatment option for RA, and evaluating the extent of degeneration of the ACL may prove important in determining its therapeutic benefits. It is also vital to visualize temporal changes in individual patients to thoroughly ascertain the state of degeneration and rupture of the cruciate ligaments, and to elucidate the mechanism of rupture. Magnetic resonance imaging, a superior diagnostic imaging technique for noninvasively visualizing soft tissue, has been reported to be useful for achieving this objective [5, 6, 7, 8, 9, 10]. However, there have been no reports of thorough investigations into degeneration of the ACL in the RA knee; therefore, we sought to elucidate the utility and limitations of Gd-enhanced MRI as a method for evaluating the ACL in the RA knee, using both surgical and histological findings to ascertain the pathological condition of the knee, and in particular, of the ACL.

Materials and methods

We studied 36 knees of 25 RA patients with ACL findings confirmed perioperatively during TKA or synovectomy. The surgical technique was TKA in 32 knees of 22 patients and synovectomy in 4 knees of 3 patients. There were 2 men and 23 women. The age at surgery ranged from 36 to 72 years (mean age 56.2 years) and the time from onset of disease to surgery ranged from 2 to 22 years (mean 13.4 years). All patients satisfied the 1987 revised diagnostic criteria of the American College of Rheumatology (formerly the American Rheumatism Association) [11]. Among these patients, histological examinations were performed for 25 knees of 20 RA patients who gave adequate informed consent before surgery, and for whom ACL findings were confirmed at TKA. This group comprised 1 man and 19 women.

The MRI equipment was a Siemens Impact 1.0-T Superconducting MRI system (Siemens, Erlangen, Germany). The pulse sequence was T1-weighted spin-echo (SE) image (TR/TE=500 ms/15 ms) and T2-weighted fast spin-echo (FSE) image (TR/TE= 4000 ms/90 ms).

Four imaging protocols were employed:

Protocol A: T1-weighted and T2-weighted sagittal images
Protocol B: T1-weighted sagittal image after infusion of Gd-DTPA (0.2 mmol/kg, i.v.)
Protocol C: T1-weighted angled coronal image, parallel to the ACL
Protocol D: T1-weighted angled coronal image, parallel to the ACL, after infusion of Gd-DTPA (0.2 mmol/kg, i.v.)

The slice thickness was set at 3 mm with no gap, field of view was 180 mm, and the imaging matrix size was 256×256. The determination of sagittal image was as follows: Firstly, axial images of the femoral chondyle in which ACL inserts into the femur were obtained; then the parasagittal direction 10° oblique from the midsagittal direction of the knee joint, which was considered to be parallel to the ACL, was determined. If the ACL was not depicted as a continuous low-intensity band, we changed the parasagittal angle to a maximum of 20°and tried again [12, 13, 14]. Next the determination of angled coronal image was coronal image, parallel to the ACL.Gd-DTPA (0.2 mmol/kg.) was injected intravenously after protocol A and protocol B. The total examination time was approximately 40–50 min.

Surgical and MRI findings of the ACL were classified into four types:

Type I (normal group): the thickness of the ACL is almost normal, and adequate tension is maintained (surgical findings), and the ACL had thick and a more complex appearance with a homogeneous signal intensity and well-defined borders (MRI findings)

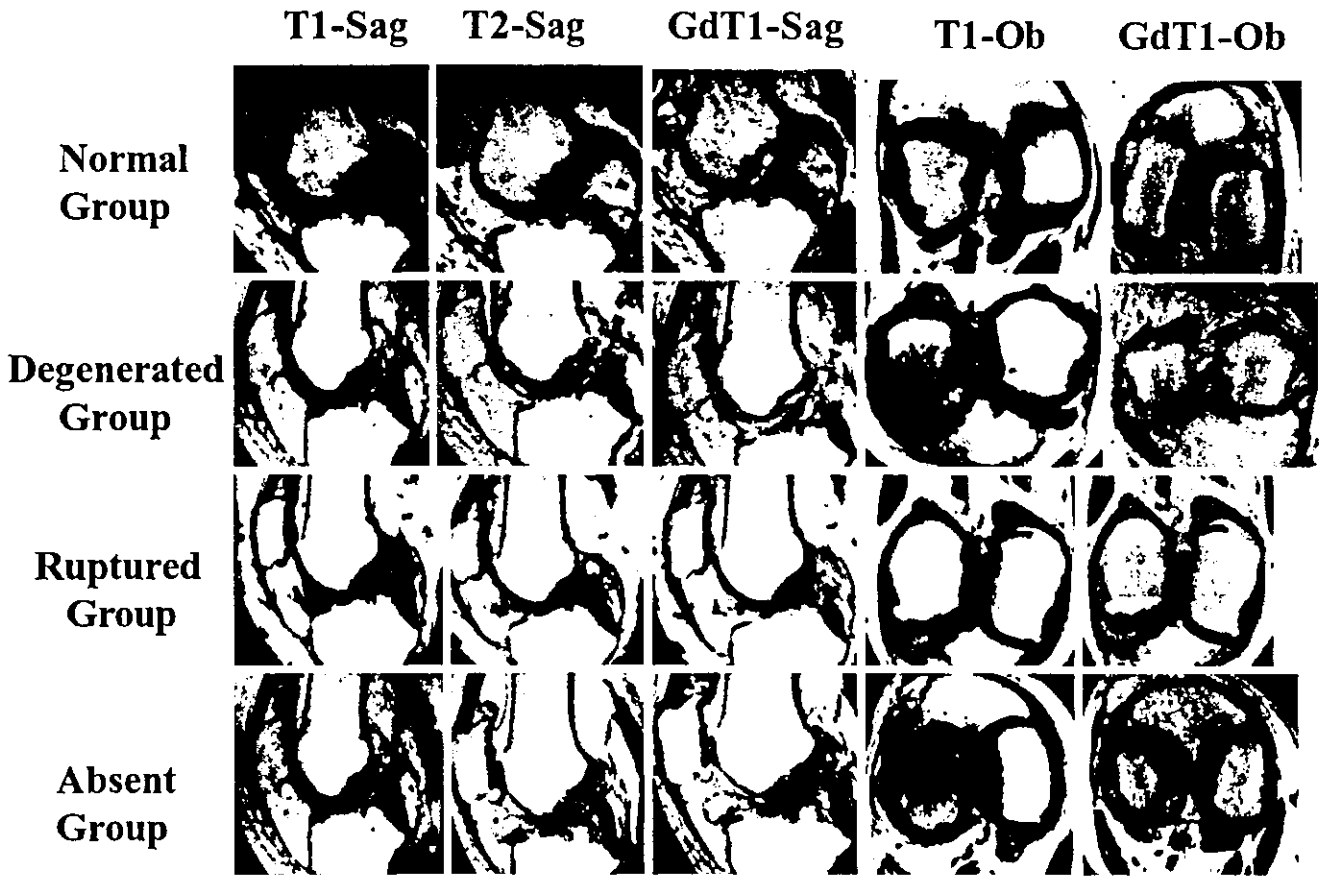

Fig. 1 The MRI findings of anterior cruciate ligament (ACL). The MRI findings of the ACL were classified into four groups. Type I (normal group): the ACL had thick and a more complex appearance with a less homogeneous signal intensity and less well-defined borders. Type II (degenerated group): the ACL had thin and a more complex appearance with a less homogeneous signal intensity and less well-defined borders. This appearance was more evident on Type II than Type I. Type III (ruptured group): the ACL appears as partial lack of low signal intensity. Type IV (absent group): the ACL appears as complete lack of low signal intensity. *Sag* sagittal, *Ob* oblique

Type II (degenerated group): the ACL has degenerated and tension is reduced (surgical findings), and the ACL had thin and a more complex appearance with a less homogeneous signal intensity and less-well defined borders. This appearance was more evident on Type II than Type I (MRI findings)

Type III (ruptured group): the parenchyma of the ACL remains but lacks continuity (surgical findings), and the ACL appears as partial lack of low signal intensity (MRI findings)

Type IV (absent group): the parenchyma of the ACL is practically absent (surgical findings), and the ACL appears as complete lack of signal low signal intensity (MRI findings; Fig. 1)

The samples of ACL obtained at surgery were fixed in 10% formalin. Subsequently, they were cut into short strips, and tissue specimens were prepared and stained with hematoxylin and eosin before histological examination. In this study, ACL was evaluated histologically at the portion of midsubstance.

Histological findings of the ACL were classified into the following two groups (Fig. 2):

Type I (normal group): almost no disorientation of collagen fibers of the ACL

Type II (degenerated group): the collagen fibers of the ACL are disorientated

Two radiologists and two pathologists who were blinded to the patients' background independently judged the MR imaging and the histological findings. If the results were divided, we decided that a third radiologist or pathologist could judge; however, practically this was not the case.

Statistical analyses were performed using Mann-Whitney U test with the threshold of significance set at 0.05.

Results

Analysis of the surgical findings of the 36 RA knees disclosed 6 knees classified as Type I, 19 knees as Type II, 7 knees as Type III, and 4 knees as Type IV (Table 1).

For each of the MR imaging protocols, we investigated the extent to which the pathological state of the knee, and primarily that of the ACL, could be accurately ascertained. Comparison of surgical and MRI findings in RA knees revealed the following:

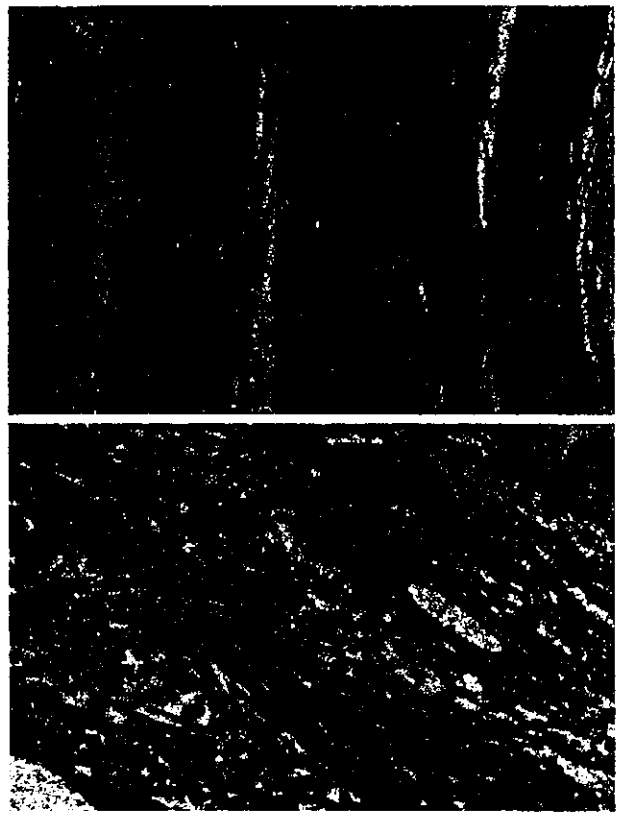

Fig. 2 Histological findings of ACL. Histological findings of the ACL were classified into the following two groups: Type I (normal group), almost no disorientation of the collagen fibers of the ACL; Type II (degenerated group), the collagen fibers of the ACL were disorientated

Table 1 Surgical findings of the anterior cruciate ligament (ACL) in rheumatoid arthritis (RA) knees

Group	Surgical findings
Normal group (Type I)	6
Degenerated group (Type II)	19
Ruptured group (Type III)	7
Absent group (Type IV)	4

Table 2 Concordance rate between surgical and MRI findings of normal group (Type I) in RA knees

	Imaging protocol			
	A	B	C	D
Concordance	4	5	2	6
Discordance	2	1	4	0
Concordance rate	4 of 6	5 of 6	2 of 6	6 of 6

Protocol A vs B: not significant; protocol A vs C: not significant; protocol C vs D: not significant; protocol B vs D: not significant

MRI findings in Type I (normal group): under imaging protocol A, the concordance rate between surgical and MRI findings was 4 of 6 (66.7%), under imaging protocol B it was 5 of 6 (83.3%), under imaging protocol C it was 2 of 6 (33.3%), and under imaging protocol D it was 6 of 6 (100%; Table 2)

MRI findings in Type II (degenerated group): under imaging protocol A, the concordance rate between surgical and MRI findings was 6 of 19 (31.6%), under imaging protocol B it was 13 of 19 (68.4%), under imaging protocol C it was 5 of 19 (26.4%), and under imaging protocol D it was 15 of 19 knees (78.9%; Table 3)

MRI findings in Type III (ruptured group): under imaging protocol A, the concordance rate between surgical and MRI findings was 1 of 7 (14.3%), under imaging protocol B it was 3 of 7 (42.9%), under imaging protocol C it was 2 of 7 (28.6%), and under imaging protocol D it was 5 of 7 knees (71.4%; Table 4)

MRI findings in Type IV (absent group): under imaging protocols A--D, the concordance rate between surgical and MRI findings was 4 of 4 (100%) (Table 5)

Significant differences between imaging protocols A and B ($p<0.05$) and imaging protocols C and D ($p<0.01$), with respect to ACL degenerated group, were recognized. But significant differences between imaging pro-